

Republic of Iraq
Ministry of Higher Education and Scientific Research
University of Kerbala
College of Medicine
Department of Microbiology



***In vitro* Effect of Caspofungin-Silver Nanoparticles on Dermatophytosis**

A Thesis

**Submitted to the Council of the College of Medicine, University of Kerbala, in
Partial Fulfillment of the Requirements for the Master
Degree in Medical Microbiology**

By

Sura Hameed Mohammed K. Al.Zubaidi

B.Sc. College of Science, Department of Biology, University of Kerbala

Supervised by

Prof. Dr. Ali Abdul Hussein S. AL-Janabi

Assist. prof. Dr. Atheer Hameid Odda Alghanimi

2024 A.D

1446 A.H

بِسْمِ اللَّهِ الرَّحْمَنِ الرَّحِيمِ

﴿ وَعَلَّمَكَ مَا لَمْ تَكُن تَعْلَمُ ﴾

صدق الله العظيم

سورة النساء: ١١٣

Supervisor Certification

We certify that this thesis entitled (*In vitro* Effect of Caspofungin-Silver Nanoparticles on Dermatophytosis) was prepared under our supervision at the College of Medicine, University of Kerbala, as a partial fulfillment of the requirements for the Degree of Master in Medical Microbiology.



Professor

Dr. Ali Abdul Hussein S. Al-Janabi
University of Kerbala
College of Medicine
Department of Microbiology
Biochemistry

Supervisor



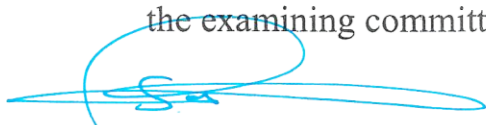
Assistant Professor

Dr. Atheer Hameid O. Alghanmi
University of Kerbala
College of Medicine
Department of Chemistry and

/ 7/2024

Chair of Microbiology Department

In view of the available recommendation, I forward this thesis for debate by the examining committee.



Prof. Dr. Sawsan Mohammed J. Al-Hasnawi

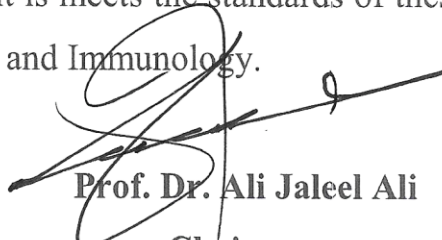
Head of Microbiology Department
College of Medicine
University of Kerbala

/ 7/2024

Committee certification

We, the examiners committee, certify that we've read the M.Sc. thesis entitled:
"In vitro Effect of Caspofungin-Silver Nanoparticles on Dermatophytosis"

We have examined the student (**Sura Hameed Mohammed Al-Zubaidi**) in its contents. In our opinion it meets the standards of thesis for the degree of Masters in Medical Microbiology and Immunology.



Prof. Dr. Ali Jaleel Ali
Chairman



Prof. Dr. Ali Tareq
Member



Assist. Prof. Dr. Alaa Abas Fadel
Member



Prof. Dr.
Ali Abdul Hussein S. Al-Janabi
Member-Supervisor

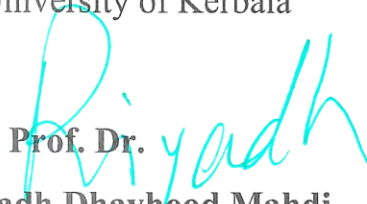


Assist Prof. Dr.
Atheer Hameid Alghanimi
Member- Supervisor

Approved by the council of the College of Medicine / University of Kerbala



Prof. Dr.
Swasan Mohammed Jabbar
Head of Microbiology Department
University of Karbala



Prof. Dr.
Riyadh Dhayhood Mahdi
Dean of Collage of Medicine
University of Karbala

/7/ 2024

/ 7/2024

Dedication

To the Present always with me.....Al-Hajjah

Al-Mahdi (AS)

To my Spiritmy great father

To my Queen.....my mother

To stars my Life.....my sisters

To my prince..... Ameer

To my AngelMyan

Sura H.

2024

Acknowledgement

First, I would like to express my thanks and gratitude to **my great Allah**. I always thank God for preparing this path and making it easy for me.

All thanks, gratitude and appreciation to my professor, mentor and supervisor, **Prof. Dr. Ali Abdul Hussein S. Al-Janabi** for his support, guidance, continuous follow-up and all the knowledge he gave me, and his effort put in to accomplish this work.

I would also like to extend my thanks and appreciation to my supervisor **Assist. Prof. Dr. Atheer Hameid O. Alghanimi**, Head of the Chemistry and Biochemistry Department in the College of Medicine, University of Kerbala, for his support, assistance, and facilitating the completion of this project in the graduate laboratory.

I would like to express my thanks and appreciation to **Prof. Dr. Sawsan Mohammed J. Al-Hasnawi**, Head of the Microbiology Department in the College of Medicine, University of Karbala, for allowing work in the graduate research laboratory and his efforts to facilitate obstacles during this project.

I would like to express my thanks and appreciation to **Dr. Sadiq Jaafar** and other staff of the Medical Consultant Dermatology at Al-Hussein Medical City Hospital.

Also, I would like to extend my thanks and appreciation to **all participating patients** and their families.

All thanks and appreciation to **Dr. Karar Al-Moussawi, Younis Hashem, Akram Joda** and my colleague **Mustafa Qahtan**.

Finally, I would like to express my thanks, gratitude and appreciation to my beloved father **Hameed M. Khadran** and my Family for their continuous support.

Sura H.

2024

Summary

Dermatophytosis is a refractory skin infection caused by dermatophytes. Caspofungin (CAS) as one of the echinocandins is one candidate to be an effective treatment for dermatophytosis. Two prepared nanoparticles forms of caspofungin with silver, including silver-caspofungin nanoparticles (Ag@Cas NPs) and chemically modified silver-caspofungin nanoparticles (modified Ag@Cas NPs), were *in vitro* evaluated in this study against dermatophytes. Chemical characteristics of these preparations were analyzed using scanning electron microscopy (SEM), dynamic light scattering (DLS) with zeta potential, ultraviolet-visible- (UV-vis) spectroscopy, Fourier transform infrared spectroscopy (FT-IR), and X-ray diffraction (XRD). Seven species of dermatophytes from 100 patients during visiting dermatological consultation of the AL-Hussein Medical City, including three species of *Microsporum* (*M. canis*, *M. ferrugineum* and *M. gypseum*) and four species of *Trichophyton* (2 *T. mentagrophytes* and 2 *T. indotineae*), were isolated from 7 patients (3 males and 4 females) with various types of dermatophytoses. Species were diagnosed based on morphological characters and molecular analyses using internal transcribed spacer *ITS1* and *ITS 2* regions sequencing of rDNA. Antifungal activities of newly prepared nanoparticle forms were evaluated using disk diffusion methods. Minimum inhibitory concentration (MIC) was also identified by the broth dilution method.

Based on chemical analysis of caspofungin nanoparticles forms, Ag@Cas NPs had more suitable characteristics as a nanoparticles compared to the modified Ag@Cas NPs. The UV spectra of Ag@Cas NPs were at 350-900. The Ag@Cas NPs had a spherical external layer around AgNPs with smaller in size than the modified Ag@CasNPs. Based on DLS, the particle size of Ag@Cas NPs was higher from mean \pm 100 nm to mean \pm 250 nm than

AgNPs were mean \pm 100, while the modified Ag@Cas NPs was much more higher (400 nm). Different chemical bonds were identified by FT-IR and XRD in the Ag@Cas NPs as indicators of the loaded of CAS on the surface of AgNPs.

The Ag@Cas NPs showed more antifungal effects on dermatophytes compared to AgNPs or caspofungin alone as controls. All isolates were inhibited by Ag@Cas NPs at concentrations of 500 mg/ml and 250 mg/ml. The *M. canis*, *T. mentagrophytes-1*, *M. ferrugineum*, and *M. gypseum* were inhibited with high inhibition zone at low concentrations of Ag@Cas NPs 62.5 mg/ml with (17.2, 12.3, 6, and 10 mm, respectively). Isolates of *Trichophyton indotineae* needed high concentrations of Ag@Cas NPs to be inhibited. The MIC of Cas@AgNPs was determined at 50 mg/ml for *M. canis*, *T. mentagrophytes-1*, *M. ferrugineum* and *M. gypseum* isolates. Isolates *T. indotineae* needed MIC of 20 mg/ml while isolate *Trichophyton mentagrophytes-2* needed MIC of 500 mg/ml. On the other hand, the modified Ag@Cas NPs was less effective on dermatophytes than Ag@Cas NPs. It was effective in high concentration (500 mg/ml) on six of seven isolates. Isolate *Trichophyton mentagrophytes-2* was resistant to this nanopreparation, while *Trichophyton indotineae-2* was more susceptible.

Conclusions: Caspofungin in the form Ag@Cas NPs have more antidermatophytic activities than silver nanoparticles (AgNPs), caspofungin, and modified Ag@Cas NPs.

List of contents

Section no.	Subject	Pages no.
	List of contents	<i>I-XII</i>
	Chapter one	
	Introduction	
1	Introduction	1
	Chapter Two	
	Review of literature	
2	Review of literature	3
2.1	Dermatophytes	3
2.1.1	Dermatophytosis, challenges and prevalence	3
2.1.2	Treatment of dermatophytosis	5
2.2	Caspofungin	6
2.2.1	Caspofungin characteristics	7
2.2.2	Antifungal activities of caspofungin	8
2.2.3	Antifungal activity of caspofungin on dermatophytes	11
2.2.4	Mechanism of caspofungin action	11
2.3	Nanotechnology and its therapeutic antimicrobial applications	13

2.3.1	Antifungal activities of silver nanoparticles	14
2.3.2	Mechanism of action of AgNPs on fungi	15
2.3.3	Antifungal activities of silver nanoparticles on dermatophytes	16
2.3.4	Mechanism of action of silver nanoparticles on dermatophytes	17
2.3.5	Antifungal activities of caspofungin nanoparticles	17
Chapter Three		
Materials and methods		
3	Materials and methods	19
3.1	Materials	19
3.1.1	Apparatuses and equipment	19
3.1.2	Chemical and biological materials	22
3.1.3	Culture media	24
3.1.4	Molecular requirements	24
3.2	Methods	25
3.2.1	Media preparation	25
3.2.1.1	Sabouraud's glucose agar (SGA)	25
3.2.1.2	Sabouraud's glucose broth (SGB)	25
3.2.1.3	Sabouraud's dextrose agar(SDA)	25
3.2.1.4	Potato dextrose agar (PDA)	26

3.2.2	Preparation of reagents	26
3.2.2.1	Preparation of potassium hydroxide (20%)(KOH)	26
3.2.2.2	Rehydration of master mix	26
3.2.2.3	Preparation of caspofungin concentration	26
3.2.3	Preparation of nanoparticles	27
3.2.3.1	Synthesis of silver nanoparticles	27
3.2.3.2	Synthesis of caspofungin-silver nanoparticles	27
3.2.3.3	Synthesis of modified caspofungin-silver nanoparticles	29
3.2.4	Characterization of synthesized nanoparticles	29
3.2.4.1	Ultraviolet-visible- (UV–Vis) spectroscopy analysis	29
3.2.4.2	Scanning electron microscopy (SEM)	30
3.2.4.3	Determination of particle size distribution	30
3.2.4.4	Fourier transform infrared spectroscopy FT-IR	31
3.2.4.5	X-Ray diffraction (XRD)	31
3.2.5	Isolation of dermatophytes	31
3.2.6	Genotyping detection	32
3.2.6.1	DNA extraction	32
3.2.6.2	PCR amplification	32
3.2.6.3	Agarose gel preparation	33

3.2.6.4	Electrophoresis method	34
3.2.6.5	Sequencing of <i>ITS</i> regions	34
3.2.7	Antifungal susceptibility assay of prepared nanoparticle materials	34
3.2.8	Minimum inhibitory concentration (MIC) of prepared nanoparticle materials	35
3.2.9	Statistical analysis	36
Chapter four		
Results		
4	Results	37
4.1	Synthesis and characterization of caspofungin-silver nanoparticles	37
4.1.1	Ultraviolet-visible- (UV–Vis) spectroscopy analysis	37
4.1.2	Scanning electron microscopy (SEM)	38
4.1.3	Determination of particle size distribution	41
4.1.4	Fourier transform infrared spectroscopy FT-IR.	43
4.1.5	X-Ray diffraction (XRD)	44
4.2	Identification of dermatophytoses and dermatophytes	44
4.3	Antidermatophytic effects of Ag@Cas NPs	54
4.4	Antidermatophytic effects of modified Ag@Cas NPs	57

4.5	Minimum inhibitory concentration (MIC) of Ag@Cas NPs on dermatophytes	60
Chapter five		
Discussion		
5	Discussion	61
5.1	Synthesis and characterization of nanoparticles	61
5.1.1	Ultraviolet-visible- (UV–vis) spectroscopy analysis.	61
5.1.2	Scanning electron microscopy (SEM)	61
5.1.3	Determination of particle size distribution by DLS and Zeta-potentials	62
5.1.4	Fourier transform infrared spectroscopy FT-IR	63
5.1.5	X-Ray diffraction (XRD)	63
5.1.6	Comparison between characteristics of Ag@Cas NPs and modified Ag@Cas NPs	64
5.2	Antidermatophytic effects of Ag@Cas NPs	65
5.3	Minimum inhibitory concentration (MIC) of Ag@Cas NPs on dermatophytes	67
Conclusions		69
Recommendations		70
References		71
الخلاصة		

List of Figures

Figure No.	Title	Pages No.
Figure 2.1	Structure of caspofungin acetate	8
Figure 3.1	illustration of synthesis of Ag@Cas NPs method used used as a nano-core template to upload caspofungin on the surface by reducing silver nitrate with trisodium citrate in the presence of caspofungin	28
Figure 4.1	UV-vis –NIR spectra of AgNPs (blue line), Ag@Cas NPs (red line), modified Ag@Cas NPs (green line), Cas (black line).	37
Figure 4.2	SEM images of (a) AgNPs, (b) Ag@Cas NPs, (c) modified Ag@Cas NPs	39
Figure 4.3	Sizes distribution calculated from SEM images of (a) Ag NPs, (b) Ag@Cas NPs	40
Figure 4.4	DLS results of AgNPs (black line), Ag@Cas NPs (red line), modified Ag@Cas NPs (blue line)	41
Figure 4.5	Zeta- potentials of AgNPs (black line), Ag@Cas NPs (red line)	42
Figure 4.6	FT-IR Spectrum of synthesized Ag@Cas NPs, with structure of caspofungin	43
Figure 4.7	XRD pattern of Ag@Cas NPs	44
Figure 4.8	PCR products of <i>ITS 1</i> and <i>ITS 2</i> regions of 7 strains of	46

	dermatophytes with Ladder DNA at the middle	
Figure 4.9	Colony of <i>M. canis</i>	47
Figure 4.10	Colony of <i>T. mentagrophytes-1</i>	48
Figure 4.11	Colony of <i>M. ferrugineum</i>	49
Figure 4.12	Colony of <i>T. indotineae-1</i>	50
Figure 4.13	Colony of <i>T. indotineae-2</i>	51
Figure 4.14	Colony of <i>T. mentagrophytes-2</i>	52
Figure 4.15	Colony of <i>M. gypseum</i>	53
Figure 4.16	Zone of inhibition (mm) of Ag@Cas NPs on (A) <i>M. canis</i> , (B) <i>M. ferrugineum</i> (C) <i>M. gypseum</i> (D) <i>T.indotineae-2</i>	56
Figure 4.17	Zone of inhibition (mm) of modified Ag@Cas NPs on (A) <i>M. canis</i> , (B) <i>M. ferrugineum</i> , (C) <i>M. gypseum</i> , (D) <i>T. indotineae-1</i>	59

List of Tables

Table No.	Title	Pages No.
Table 3-1	Apparatuses used in the study	19
Table 3-2	Equipment used in the study	21
Table 3-3	Chemical and biological materials	22
Table 3-4	Already prepared culture media	24

Table 3-5	Primers sequences used for PCR	24
Table 3-6	PCR Master mix components	24
Table 3-7	The PCR condition for amplification of <i>ITS</i> regions	33
Table 4-1	Dermatophytoses with species of dermatophytes	45
Table 4-2	Effect of Ag@Cas NPs on isolated fungi using disc diffusion method	55
Table 4-3	Effect of modified Ag@Cas NPs on isolated fungi using disc diffusion method	58
Table 4-4	Minimum inhibitory concentration (MIC) of Ag@Cas NPs on dermatophytes	60

List of Abbreviations

µg/ml	Microgram per milliliter
µl	Micro liter
Ag	Silver
Ag@Cas NPs	Silver-caspofungin nanoparticles
AgNO₃	Silver nitrate
AgNPs	Silver nanoparticles
AmB	Amphotericin B
ANOVA	Analysis of variance
ATP	Adenosine triphosphate
AuNPs	Gold nanoparticles
Bio-AgNPs	Biological synthesis silver nanoparticles
BLAST	Basic Local Alignment Search Tool
bp	Base pair

CAS	Caspofungin
CAS-AuNPs	Caspofungin-golden nanoparticles
Caspofungin-ZnO NPs	Caspofungin-zinc oxide nanoparticles
Caspofungin-AgNPs	Caspofungin-silver nanoparticles
Chem-AgNPs	Chemical synthesis silver nanoparticles
CLSI	Clinical and Laboratory Standards Institute
Da	Dalton
dATP	Deoxyadenosine triphosphate
dCTP	Deoxycytidine triphosphate
dGTP	Deoxyguanosine triphosphate
DLS	Dynamic light scattering
DNA	Deoxyribonucleic acid
dNTPs	Deoxynucleotide triphosphate
dTTP	Deoxythymidine triphosphate
EDTA	Ethylene Diamine Tetra Acetic Acid
FDA	Food and Drug Administration
FKS	Fungal kinase synthase
FT-IR	Fourier transform infrared
FWHM	Full width at half maximum
GF-ZnO NPs	Griseofulvin- zinc oxide nanoparticles
GTPase	Guanosine triphosphate enzymes
IC₈₀	Inhibition concentration 80
ITS	Internal transcribed spacer
KOH	Potassium hydroxide
MEC	Minimum effective concentration
MEC90	Minimum effective concentration 90
MFC	Minimum fungicidal concentration

MgCl₂	Magnesium chloride
MIC	Minimum inhibitory concentration
MIC₉₀	Minimum inhibitory concentration 90
MIC₅₀	Minimum inhibitory concentration 50
mV	Millivolt
NAC	Non-albicans <i>Candida</i>
NCBI	National Center Biotechnology Information
nm	Nanometer
NPs	Nanoparticles
PBS	Phosphate buffer saline
PCR	Polymerase chain reaction
PDA	Potato dextrose agar
Pmol	Picomole
Psi	Pounds per Square Inch
rDNA	Ribosomal Deoxyribonucleic acid
Rho1	Ras homologous-1 gene
ROS	Reactive oxygen species
RPM	Round per minute
SD	Standard deviation
SDA	Sabouraud's dextrose agar
SEM	Scanning electron microscopy
SGA	Sabouraud's glucose agar
SGB	Sabouraud's glucose broth
Taq	<i>Thermus aquaticus</i>
TBE	Tris borate EDTA
Uv	Ultraviolet
Uv-vis	Ultraviolet-visible
Uv-vis-NIR	Ultraviolet-visible- Near Infrared

XRD	X-Ray Diffraction
ZnO	Zinc oxide
ZP	Zeta Potential

CHAPTER ONE

INTRODUCTION

1. Introduction

Dermatophytes are a wide range of pathogenic fungi using keratin as a nutrient source (Cabañes, 2020; Paryuni *et al.*, 2020). Skin, hair, and nails with keratinous materials encourages dermatophytes to cause infections called dermatophytoses or tinea on various skin parts of the human body (Suganthi, 2017; Rouzaud *et al.*, 2016). Three genera included within the dermatophytes; *Trichophyton*, *Microsporum*, and *Epidermophyton* are the main genera causing dermatophytoses and the most common genus is *Trichophyton* spp., followed by *Epidermophyton* spp. and *Microsporum* spp. (Datt and Datt, 2023).

There are several effective antifungal groups usually used for the treatment of tinea, including polyenes, azoles, allylamines, pyrimidine analogs, and echinocandins (Sucher *et al.*, 2009; Chen and Sorrell, 2007). Treatment mostly needs a long time for any of these drugs (Datt and Datt, 2023). Caspofungin which belonged to the echinocandin group was the first antifungal of echinocandin approved by the United States Food and Drug Administration (FDA) for the treatment of fungal infections (Cappelletty and Eiselstein-McKittrick, 2007). It has a fungicidal effect on *Candida* spp. and fungistatic on *Aspergillus* spp. (Gil-Alonso *et al.*, 2019). Antifungal activities of echinocandin on dermatophytes have been approved by a few studies (Su *et al.*, 2023). Caspofungin showed antidermatophytic action on three species of dermatophytes (*T. rubrum*, *T. violaceum*, and *T. tonsurans*) at minimum effective concentration MEC90 (0.5 µg/mL) with less effects on others such as *M. canis*, *M. gypseum*, *T. mentagrophytes*, and *E. floccosum* (Bao *et al.*, 2013). The mechanism of action of caspofungin on fungi is inhibiting the synthesis of cell walls by blocking the synthesis of the β -(1,3)-D-glucan (Pacifici, 2020).

A new line of materials in the nanoscale called nanoparticles have been synthesized in size of 1-1000 nm (Nagaraj *et al.*, 2021; Kischkel *et al.*, 2020). They showed antimicrobial actions on various groups of pathogens due to their

physicochemical characteristics (Castillo *et al.*, 2018). Nanotechnology improve stability, drug solubility and bioavailability. Metallic nanoparticles such as silver nanoparticles (AgNPs) are the common type of nanomaterials that is used against several pathogenic fungi (Castillo *et al.*, 2018). The antifungal activities of AgNPs on dermatophytes were variable between effective and ineffective. Clinical isolation of *T. mentagrophytes* was inhibited by 1-7 µg/ml of AgNPs, which is equal to the activity of amphotericin B (AmB) and more than fluconazole (Kim *et al.*, 2008). Meanwhile, *M. canis*, *T. mentagrophytes*, and *M. gypseum* were less affected by AgNPs compared to griseofulvin (Mousavi *et al.*, 2015). The main sites of fungal cells affected by AgNPs are cellular membranes and cell walls (Essghaier *et al.*, 2022). A combination of caspofungin with metallic nanoparticles was found in only two studies on *Candida* spp. and not on dermatophytes. The first one was the effect of caspofungin with synthetic golden nanoparticles (CAS-AuNPs) (Salehi *et al.*, 2021). The second was caspofungin combined with zinc oxide nanoparticles on *C. auris* (Fayed *et al.*, 2021).

Aims of the study:

1. To prepare caspofungin in different nanoparticles forms using silver nanoparticles as a template.
2. To prove *in vitro* evaluation of the antifungal efficacy of caspofungin-silver nanoparticles against dermatophytes comparing to commercial caspofungin and AgNPs as control.

Chapter Two

*Review of
Literature*

2. Review of literature

2.1 Dermatophytes

Dermatophytes are a member of pathogenic fungi living on the keratinous part of the human body like skin, hair, and nails (Cabañes, 2020; Paryuni *et al.*, 2020). Keratin is fibrous protein the main nutrient for dermatophytes due to their ability to produce keratinase allow to invade keratin tissue (Paryuni *et al.*, 2020). The availability of keratin in the upper cutaneous layer makes infection with dermatophytes restricted within this layer of skin (Jonhson, 2003).The hyphae with arthrospores are the usual forms of dermatophytes on the skin (Jonhson, 2003).

The primary habitat for dermatophytes are animals, humans, and soil (Paryuni *et al.*, 2020; Cabañes, 2020). Dermatophytes involve about 42 different species (Al-Khikani, 2020). These species belong to three genera; *Trichophyton*, *Epidermophyton*, and *Microsporum* (Cabañes, 2020; Shweta and Manju, 2018). The genus *Trichophyton* includes 24 species, *Microsporum* 16 species and *Epidermophyton* has 2 species (Datt and Datt, 2023).

2.1.1 Dermatophytosis, challenges and prevalence

The infection caused by dermatophytes is called dermatophytosis (Suganthi, 2017; Rouzaud *et al.*, 2016). Different species of dermatophytes can cause dermatophytosis which is the most common fungal skin infection with a high prevalence rates (20-25%) all over the world (Cabañes, 2020). Tinea is another name for dermatophytosis (Martinez-Rossi *et al.*, 2018). The keratinized tissues of the skin, nails, and hair are most affected by dermatophytic infection (Cabañes, 2020; Paryuni *et al.*, 2020). Many factors can affect dermatophytosis development include that relate to the fungi such as the species of dermatophytes, and type of virulence factor, or relate to the human such as age,

immune state, and sex (Paryuni *et al.*, 2020). The other factors related to the human sociocommunity also assist dermatophytosis such as overcrowding, poor hygiene, contact with animals, and dressing in tight clothes (Al-Khikani, 2020). The predominant cause of dermatophytosis is mainly by *Trichophyton* spp. followed by *Epidermophyton* spp. and *Microsporum* spp. (Datt and Datt, 2023). *Epidermophyton floccosum* and *Trichophyton rubrum* are infected skin cells only, while *Trichophyton mentagrophytes* and *Trichophyton tonsurans* can infect skin cells, hairs, and nails (Al-Janabi, 2014).

The dermatophytosis or tinea can take different names based on the location on the human body, such as tinea capitis (head), tinea corporis (glabrous skin), tinea cruris (genital regions), and tinea pedis (foot) (Datt and Datt, 2023). The source of infection can be from infected humans (anthropophilic) such as *Epidermophyton floccosum*, animals (zoophilic) such as *M. canis*, or soil (geophilic) such as *M. gypseum* (Datt and Datt, 2023; Brescini *et al.*, 2021). Zoophilic and geophilic groups cause more acute and inflammatory infections in humans (Brescini *et al.*, 2021). The dermatophytosis lacks or rarely causes death when major of them cause mild symptoms of skin infection and a few cases with invasive infection (Kidd and Weldhagen, 2022; Brescini *et al.*, 2021).

In Iraq, the prevalence and incidence of dermatophytosis are high enough to consider this infection more common in many Iraqi provinces (Sharquie and Jabbar, 2021). Tinea corporis and tinea capitis have the highest infection rates in Al-Nassiriyah City, while the lowest one was tinea faciei (Najem *et al.*, 2016). Females were more infected by these types of tinea (67.27%) than males (32.73%). The same results were also recorded in Kirkuk City where tinea corporis was a high rate in contrast to tinea facial and the incidence of infection was higher in the city than in the countryside (Abdulkareem *et al.*, 2022). In Hilla City, tinea unguium (onychomycosis) and tinea cruris were the most

prevalent dermatophytoses (22.5% of each) compared to tinea manuum (hands) (1%) and tinea faciei (4%) and the rate in rural was more than in urban sites (Abed Ali *et al.*, 2017). Another study in Hilla City also showed that tinea unguium (32.63%) is more prevalent dermatophytoses (Hindy and Abiess, 2019). Tinea capitis (47.5%) and tinea cruris (32.5%) in Baghdad City were the predominant types of tinea corporis (20%), especially in children less than 10 years (Mohammed *et al.*, 2015). In Karbala City, tinea capitis and tinea pedis were the most prevalent in both males and females compared to tinea cruris which was found in males only (Al-Janabi and Mohamed, 2021). In contrast, tinea capitis (15%) was the low rate type of dermatophytosis in Basra City compared to high rates of tinea corporis (50%) and tinea pedis (25%) (Alatbee *et al.*, 2021).

2.1.2 Treatment of dermatophytosis

The treatment of dermatophytosis usually takes a long time ranging from weeks to a year depending on the type of tinea (Datt and Datt, 2023). Some infections consider recalcitrant and it is difficult to treat as with some cases of tinea corporis and tinea cruris (Khurana *et al.*, 2019). Factors of infection site, causative agent, and pharmacokinetics of drugs usually affect the efficacy of the treatment (Datt and Datt, 2023).

Generally, antifungal drugs for dermatophytoses are used in many forms such as topical or systemic-oral forms (Brescini *et al.*, 2021). Topical drugs are more safe and effective than systemic antifungals (Al-Khikani, 2020), but this is not always true with cases of tinea capitis and onychomycosis, which are often not affected by topical drugs (Hainer, 2003). On the other hand, treatment of tinea pedis with topical antifungals results in curing within 4-8 weeks (Suganthi, 2017). However, systemic therapy is more needed for the treatment of refractory cases of dermatophytoses (Hainer, 2003).

The five main classes of antifungals that are commonly used for the treatment of fungal infections include polyenes, azoles, allylamines, pyrimidine analogs, and echinocandins (Sucher *et al.*, 2009; Chen and Sorrell, 2007). Antifungal like griseofulvin is not related to any of these classes, but it has fungistatic action on all of dermatophytosis with a long duration of treatment (Datt and Datt, 2023). The duration of the treatment course of antifungals may be shorter as with topical allylamines or often higher as with azoles (Hainer, 2003). However, the azole antifungals, such as clotrimazole, miconazole, and econazole are generally used for the treatment of dermatophytoses (Brescini *et al.*, 2021). Some azoles such as the broad spectrum activity of the triazole group have more therapeutic actions with better safety profile compared to the imidazole group (Khurana *et al.*, 2019). Agents from the allylamine family, such as terbinafine and naftifine, are also used (Brescini *et al.*, 2021). Badiee *et al.*, (2023) found that terbinafine with luliconazole and isavuconazole were *in vitro* effective against 198 isolates of dermatophytes.

2.2 Caspofungin

The new antifungal compounds are very slowly developed and even those which were discovered are faced difficulty in proving their clinical therapeutic activities on fungal infections. Caspofungin is a new antifungal that belongs to the echinocandin antifungal class. Many of echinocandins field to receive approval from the United States Food and Drug Administration (FDA) for the treatment of fungal infections. Caspofungin was the first one approved to be used clinically in January 2001 (Szymanski *et al.*, 2022; Hashemian *et al.*, 2020). After caspofungin, micafungin, and anidulafungin were received such approval later (Song and Stevens, 2015). Caspofungin acetate was the form of caspofungin marketed after FDA approval under the name of CANCEL[®] (Kartsonis *et al.*, 2003).

Caspofungin is not a chemical synthesis product at the first time of discovery. It was isolated as natural product from the fungus *Glarea lozoyensis* (Bellmann and Smuszkiewicz, 2017; Song and Stevens, 2015). Later, it was synthesized by the condensed research of Merck Research Laboratories to hold the name of MK-0991 or L-743.872 (Kartsonis *et al.*, 2003; Letscher-Bru and Herbrecht, 2003; Stone *et al.*, 2002). The trademark of caspofungin acetate nowadays is CANCIDAS[®], Merck & Co. Inc. Whitehouse Station, N.J., USA (Bellmann and Smuszkiewicz, 2017).

2.2.1 Caspofungin characteristics

Caspofungin is a semisynthetic derivative of pneumocandin B₀, which is naturally occurring as a lipopeptide cyclic (Szymanski *et al.*, 2022; Nagaraj *et al.*, 2021). The chemical structure of caspofungin is 1[(4R,5S)-5-[(2-aminoethyl)amino]-N2-(10,12-dimethyl-1-oxotetradecyl)-4-hydroxy-Lornithine]-5-[(3R)-3-hydroxy-L-ornithine] pneumocandin B₀ diacetate (**Figure 2.1**) (Song and Stevens, 2015). The chemical formula of caspofungin acetate is C₅₂H₈₈N₁₀.O₁₅. 2C₂H₄O₂ with a molecular weight of 1213 Da (Hashemian *et al.*, 2020). Antifungal activity of caspofungin acetate is related to the cyclic hexapeptide core linked to an N-linked fatty acyl side chain (Bellmann and Smuszkiewicz, 2017). Caspofungin acetate is a white to off-white powder and soluble in water and methanol with limited solubility in ethanol (Kofla and Ruhnke, 2011; Hope *et al.*, 2007).

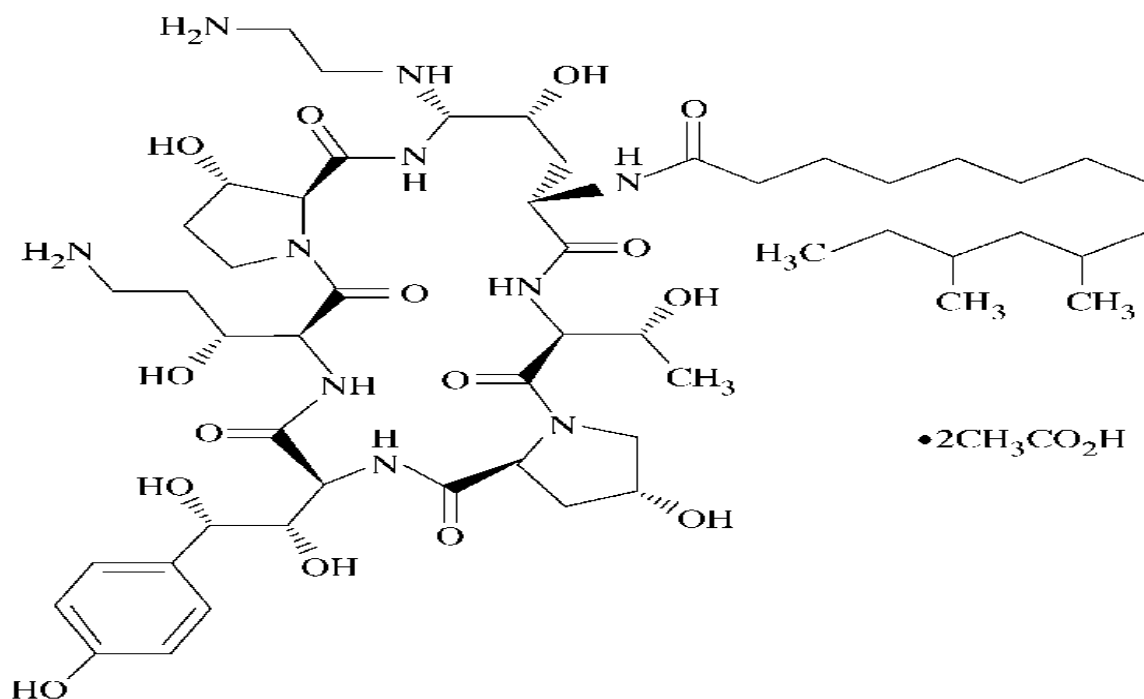


Figure 2.1: Structure of caspofungin acetate (Letscher-Bru and Herbrecht, 2003)

Caspofungin acetate is produced for use as a parenteral drug, particularly as an intravenous infusion due to its lack of oral bioavailability, its poor tissue penetration and low lipophilicity as limitation of caspofungin (Song and Stevens, 2015). White lyophilized powder in a vial containing 50 to 70 mg is the commercially available form of caspofungin acetate to be given by intravenous infusion over 1 hour (Song and Stevens, 2015). Caspofungin has a perfect safety profile with reduced toxicities and high tolerability compared with other antifungals (Balkovec *et al.*, 2014). It also has fewer adverse effects with few drug interactions (Hashemian *et al.*, 2020).

2.2.2 Antifungal activities of caspofungin

Antifungal groups rather than echinocandins have many troubles therapeutic characteristics such as the toxicity of polyenes, limited oral absorptions and low antifungal activities of most azoles, and resistance to antifungal as with flucytosine (Jonhson and Perfect, 2003). The absence or

diminishing of these characteristics in echinocandins, including caspofungin, promotes to use of this group as the first line against many severe fungal infections (McCormack and Perry, 2005). Caspofungin is preferred now for the treatment of infections of *Candida* spp. and *Aspergillus* spp. (Szymanski *et al.*, 2022). It has fungicidal action on *Candida* spp. and fungistatic action on *Aspergillus* spp. (Gil-Alonso *et al.*, 2019).

The minimum inhibitory concentration (MIC) of caspofungin has been identified only on *Candida* spp., but not on filamentous fungi (Song and Stevens, 2015). The MIC on *Candida* spp. was determined in ≤ 1 $\mu\text{g/ml}$ based on laboratory *in vitro* studies and upon clinical measurement of caspofungin concentration in serum (Jonhson and Perfect, 2003). Several studies approved the antifungal activity of caspofungin on different species of *Candida*, including *C. albicans*, *C. glabrata*, *C. tropicalis*, *C. dubliniensis*, and *C. krusei* based on *in vitro* and *in vivo* experiments (Kofla and Ruhnke, 2011). Some species of *Candida*, such as *C. glabrata* may be less affected by caspofungin compared to micafungin based on *in vitro* studies, but these effects increased to become the same by these antifungals after *in vivo* study (Yamada *et al.*, 2016). Other studies found non-significant differences between caspofungin and anidulafungin or micafungin in MIC against *C. glabrata* (Song and Stevens, 2015). Caspofungin has also effective antifungal activity against clinical isolates of *C. albicans* and non-albicans *Candida* (NAC), including azole-resistant strains (Jonhson and Perfect, 2003). Some species of *Candida* showed less affected by caspofungin such as *C. parapsilosis*, *C. guilliermondii*, and *C. lusitaniae* (Wiederhold and Herrera, 2012). Pfaller *et al.* (2006) found that 98.2% of *Candida* spp. were inhibited by caspofungin in MIC < 0.5 $\mu\text{g/ml}$ and 99.7% in MIC < 1 $\mu\text{g/ml}$ with MIC₅₀ of 0.03 $\mu\text{g/ml}$ and MIC₉₀ of 0.25 $\mu\text{g/ml}$.

Caspofungin has antifungal activity on many species of filamentous fungi more specifically on *Aspergillus* spp. (Agarwal *et al.*, 2006). Its activities included species of *A. fumigatus*, *A. flavus*, *A. niger*, and *A. terreus* (Jonhson and

Perfect, 2003). Other filamentous fungi showed variables affected by caspofungin depending on species and it could be poor activity against most filamentous fungi *in vitro* (Jonhson and Perfect, 2003). Caspofungin is active against *Paecilomyces variotii* (MIC ≤ 0.5 mg/L) (Song and Stevens, 2015) and *Penicillium* sp. (Cappelletty and Eiselstein-McKitrick, 2007). It also has antifungal action on several species of dimorphic fungi like *Histoplasma capsulatum*, *Coccidioides immitis*, *Blastomyces dermatitidis*, and *Sporothrix schenckii* (Cappelletty and Eiselstein-McKitrick, 2007). The MIC values of caspofungin in *B. dermatitidis* and *H. capsulatum* are 2 and 1.3 $\mu\text{g/ml}$, respectively with low activity on *S. schenckii* (5.4 $\mu\text{g/ml}$) (Jonhson and Perfect, 2003). However, echinocandins have variable activity on the dimorphic fungi depending on the growth state of the organism (Cappelletty and Eiselstein-McKitrick, 2007). Some types of fungi are not affected by caspofungin such as *Cryptococcus neoformans* and *Fusarium* species (Wiederhold and Herrera, 2012), and the causative agents of mucormycosis (e.g., *Rhizopus* spp., *Rhizomucor* spp., and *Cunninghamella* spp. (Wiederhold and Herrera, 2012).

Many *Candida* infections (candidiasis) and aspergillosis have been treated by caspofungin such as candidemia, candidiasis in the esophagus and peritonea, and treatment of neutropenic patients or those with abdominal Candidal abscesses (Song and Stevens, 2015; Zhang *et al.*, 2014). Caspofungin is the only member of echinocandins approved for use as a therapy for patients with invasive aspergillosis who have shown refractoriness (Song and Stevens, 2015). Infections with pulmonary aspergillosis in both normal and immunocompromised animal models demonstrated the efficacy of caspofungin as a therapeutic agent (Groll and Walsh, 2001). In general, caspofungin has many advantageous characters to other antifungals including high efficacy in treating fungal infection (15% superior to fluconazole); mild symptoms; and absence of antagonism in combination with other antifungal drugs (Zhang *et al.*, 2014).

2.2.3 Antifungal activity of caspofungin on dermatophytes

Although few studies are performed to detect the antifungal activities of echinocandins on dermatophytes, echinocandins have been demonstrated to have *in vitro* activity against many species of dermatophytes and could be considered options for the treatment of dermatophytoses (Su *et al.*, 2023). Species of *T. rubrum*, *T. violaceum*, and *T. tonsurans* were more affected by caspofungin at MEC₉₀ (0.5 µg/mL) compared to *M. canis*, *M. gypseum*, *T. mentagrophytes*, and *E. floccosum* (Bao *et al.*, 2013). Although micafungin and anidulafungin had more effects than caspofungin on *T. rubrum* isolates, a total of 35 isolates of *T. rubrum* were inhibited by caspofungin at a minimum effective concentration (MEC) of 0.5 mg/L (Su *et al.*, 2023). Caspofungin in combination with antidepressant sertraline showed antifungal activity against *T. rubrum* and its biofilm (Rocha *et al.*, 2022).

2.2.4 Mechanism of caspofungin action

The cell walls of pathogenic fungi such as *C. albicans* and *A. fumigatus* are rigid structures composed of β-(1,4)-D-glucan, β-(1,3)-D-glucan, β-(1,6)-D-glucan, mannan or galactomannan, and chitin, along with glycoproteins and α-glucans (Song and Stevens, 2015). Caspofungin as well as other echinocandins inhibit the synthesis of the β-(1,3)-D-glucan which is one component of the fungal cell wall (Pacifici, 2020; Perlin, 2015). The main function of the β-(1,3)-D-glucan is to maintain cellular integrity by providing osmotic stability (Szymanski *et al.*, 2022; Pacifici, 2020). Other functions are associated with cell growth and cell division (Groll and Walsh, 2001). However, targeting of caspofungin to the cell wall of fungal cells, which does not occur in mammalian cells, makes caspofungin an excellent antifungal for fungal cells without any harm to human cells (Wiederhold and Herrera, 2012).

Mechanism of action of caspofungin in the synthesis of β -(1,3)-D-glucan of the fungal cell wall may take fungistatic or fungicidal effects (Nagaraj *et al.*, 2021; Hashemian *et al.*, 2020). A fungistatic effect is performed by reducing the rate of cell growth due to the inhibition of cell wall synthesis (Nagaraj *et al.*, 2021; Hashemian *et al.*, 2020). In contrast, the fungicidal effect is represented by the complete blockage of the cell wall synthesis (Letscher-Bru and Herbrecht, 2003). The activity of caspofungin on mold such as *Aspergillus* spp. is usually fungistatic with more specificity by targeting the cells of the tips and branches of growing hyphae (Hashemian *et al.*, 2020). On the other hand, caspofungin acts as a fungicidal agent on yeast like *Candida* spp. by weakening the mechanical strength of the cell wall. Such weakness leads to a burst of fungal cells under the effects of internal high osmotic pressure (Nagaraj *et al.*, 2021; Hashemian *et al.*, 2020).

The site of action of caspofungin to inhibit the synthesis of β -(1,3)-D-glucan is by targeting the enzyme β -(1,3)-D-glucan synthase (Hashemian *et al.*, 2020). This enzyme is composed of two subunits; Fungal kinase synthase *FKS* and Ras homologous-1 gene *Rho1*. (Kofla and Ruhnke, 2011; Stone *et al.*, 2002). The active subunit is *FKS*, which is encoded by three genes; *fKs1*, *fKs2*, and *fKs3* (Kofla and Ruhnke, 2011), while the *Rho1* subunit which belongs to the Guanosine triphosphate enzymes GTPase family has a regulatory function (Szymanski *et al.*, 2022). Of the three encoded proteins of *FKS*, *FKS1* is the most important one in the synthesis of β -(1,3)-D-glucan, which is mainly targeted by caspofungin and other echinocandins (Hashemian *et al.*, 2020).

In comparison with other antifungal groups, resistance to echinocandins is still rare (Kofla and Ruhnke, 2011). A few cases have recently indicated emerging resistance to caspofungin with more specificity among species of *Candida* (Song and Stevens, 2015). Resistance to caspofungin may result from a mutation in the fungal genome or alteration in the structure of the fungal cell wall (Pacifici, 2020). Thus, fungi can always activate adaptive mechanisms that

induce cell wall repair (Szymanski *et al.*, 2022). Resistance by mutation is mainly developed in the FKS subunit of the β -(1,3)-D-glucan synthase (Szymanski *et al.*, 2022). Such mutation responsible for resistance to caspofungin has been *in vitro* demonstrated in the strains of *Saccharomyces cerevisiae* and *C. albicans*, which are still susceptible to azoles and amphotericin B (AmB) (Letscher-Bru and Herbrecht, 2003).

2.3 Nanotechnology and its therapeutic antimicrobial applications

Nanotechnology is a technique of using materials that have nanoparticles (NPs) in size of 1-1000 nm (Nagaraj *et al.*, 2021; Kischkel *et al.*, 2020). Such a technique has recently been applied in different industrial and medical fields. Creating NPs within the size of 1-100 nm has been proved by several studies to have effective therapeutic activities through the synthesis of new formulas of antimicrobial agents (Carmo *et al.*, 2023; Castillo *et al.*, 2018). Enhancement of drug delivery and works as a detection system for biological and chemical agents are other functions of NPs (León-Buitimea *et al.*, 2021; Gürsu, 2020). The physicochemical characteristics of NPs are the main reason for successful of these NPs as therapeutic agents or carriers (Castillo *et al.*, 2018). In fact, the small size of NPs has higher antimicrobial activities than larger NPs due to fast entry to the cells (Carmo *et al.*, 2023). The toxicity and side effects of NPs are few compared to other antimicrobial agents (León-Buitimea *et al.*, 2021; Nagaraj *et al.*, 2021; Gürsu, 2020). The NPs also can pass biological barriers in the human body (León-Buitimea *et al.*, 2021). The advantages of NPs to antifungals include their ability to enhance the therapeutic characteristics of these agents by increasing their aqueous solubility, bioavailability, and treatment efficacy (León-Buitimea *et al.*, 2021; Gürsu, 2020; Soliman, 2017). Resistance to antifungals can also be reduced by using nanoparticle preparations (Nagaraj *et al.*, 2021). In general, many factors can affect the NPs therapeutic efficacy and

degree of toxicity, including their size, shape and capping nature, aggregation, solubility, and superficial charge (Kischkel *et al.*, 2020).

Several synthetic forms of NPs are developed to be used as therapeutic agents, including metallic nanoparticles, polymers, lipid coating materials, phospholipid vesicles, non-phospholipid vesicles, solid lipid nanoparticles, nanoemulsions and dendrimers (León-Buitimea *et al.*, 2021; Soliman, 2017). Metallic nanoparticles primarily include a metals such as silver, gold, zinc or copper oxides, palladium, titanium, or magnesium oxide (Kavitha *et al.*, 2020; Kischkel *et al.*, 2020). Such types of NPs have shown antimicrobial activities against different pathogens such as fungi, bacteria, or viruses (Kischkel *et al.*, 2020).

2.3.1 Antifungal activities of silver nanoparticles

Silver nanoparticles (AgNPs) are one of the widely used metallic nanoparticles against pathogenic fungi (Castillo *et al.*, 2018). Silver ions have many properties that make them suitable to form nanoparticle formulas in addition to their ability to bind with other compounds. These characters include its good conductivity, chemical stability, catalytic and antimicrobial toxic action (Huang *et al.*, 2023; Nagaraj *et al.*, 2021).

The antifungal activities of AgNPs have been proven against different pathogenic fungi such as *Candida* spp. and *Aspergillus* spp. (Carmo *et al.*, 2023). *Candida* species are more affected by the antifungal action of AgNPs than filamentous fungi as with the causative agents of coccidioidomycosis and mucormycosis (León-Buitimea *et al.*, 2021; Perween *et al.*, 2019). Biofilm production is also inhibited by AgNPs such as that produced by *C. auris* (Huang *et al.*, 2023; AlJindan and AlEraky, 2022). The growth and biofilm production of *C. albicans* were inhibited by the synthetic metallic nanoparticles of silver,

and gold, and it demonstrated the *in vivo* efficacy on oral and cutaneous candidiasis in rodent models (Carmo *et al.*, 2023).

Minimum doses of AgNPs are usually enough to kill microorganisms including those resistant species to antibiotics with an ability to reduce virulence factors (Castillo *et al.*, 2018). Resistance isolates of *C. albicans* to many conventional antifungals were inhibited by low concentrations of AgNPs (MIC; 0.125-0.5 $\mu\text{g/ml}$) (Perween *et al.*, 2019). The AgNPs showed significant inhibition activities on two clinical strains of *C. albicans* at low MIC (0.27 $\mu\text{g/ml}$ and 0.97 $\mu\text{g/ml}$) compared to AmB (0.5 $\mu\text{g/ml}$ and 2 $\mu\text{g/ml}$) with a morphological change of cell surface of the treated cells with AgNPs (Malathi *et al.*, 2022).

The AgNPs has a significant role in increasing the antifungal activities of many conventional antifungals or other compounds after being combined with these materials. The combination of AgNPs with miconazole showed high efficacy against *C. albicans* compared to the effect of these components alone (Huang *et al.*, 2023). Synergism action against the biofilm of *C. albicans* was observed after the combination of AgNPs with fluconazole through enhancement penetration of fluconazole by NPs, while Ag affected the efficacy of efflux transporter (Kischkel *et al.*, 2020).

2.3.2 Mechanism of action of AgNPs on fungi

The mechanism of AgNPs action as an antimicrobial agent is represented by the releasing of oxidative silver ions (reactive oxygen species ROS generation) that cause damage to the cell wall and enzymatic system of the microorganism as well as their effect on gene expression and the structures of many cellular pathways and components (e.g. decreasing ATP levels, proteins and DNA) (Carmo *et al.*, 2023; Huang *et al.*, 2023). The oxidative state of AgNPs facilitates their interaction with the microbial outer membrane (Castillo

et al., 2018). Many components of *Trichosporon asahii*, including cellular outer membrane (plasma and cell wall), chromatin, mitochondria, and ribosomes were damaged after treatment with AgNPs at MIC of 0.5 µg/ml compared to high MIC of many conventional antifungals (Xia *et al.*, 2016).

2.3.3 Antifungal activities of silver nanoparticles on dermatophytes

Antifungal activities of nanoparticles, including AgNPs either alone or with other compounds, on dermatophytes have been demonstrated by many studies. A new preparation of nanoparticles formula composed of silver and zinc oxide called xerogel showed significant activities on two species of dermatophytes (*T. mentagrophytes* and *T. verrucosum*) at low MIC (3.75 µg/ml and 7.5 µg/ml, respectively) (Al-Janabi and Bashi, 2019). In contrast, the effect of AgNPs on three species of dermatophytes (*M. cans*, *T. mentagrophytes*, and *M. gypseum*) were less effective than by griseofulvin (Mousavi *et al.*, 2015). The MIC of AgNPs in that study were 200, 180, and 170 µg/ml, respectively, while griseofulvin effects by MIC 25, 100, and 50 µg/ml, respectively. Such antidermatophytic activities of griseofulvin were increased by converting it to a nanoparticle structure with zinc oxide (GF-ZnO NPs) against *T. mentagrophytes* and *T. verrucosum* compared to griseofulvin alone (Al-Janabi and Bashi, 2022).

Antidermatophytic activities of AgNPs obtained either from the extract of *Penicillium chrysogenum* and *Aspergillus oryzae* as a biological source or from chemical synthesis with a coating of polyvinylpyrrolidone were assessed on eight clinical strains and standard one of *T. rubrum* (Pereira *et al.*, 2014). AgNPs from both sources showed antifungal action on all strains of *T. rubrum*. Meantime, the biological one was more active than fluconazole but it was less than either chemical synthesis, itraconazole, or terbinafine. Kim *et al.* (2008) found that synthetic spherical AgNPs have antifungal actions on clinical and standard isolates of *T. mentagrophytes* and *C. albicans* at inhibition

concentration (IC₈₀) 1-7 µg/ml, which is close to the activity of AmB (IC₈₀, 1-5 µg/ml) and more than the activity of fluconazole (IC₈₀, 10-30 µg/ml). These AgNPs also showed activity in the mycelium form of *C. albicans*.

2.3.4 Mechanism of action of silver nanoparticles on dermatophytes

The AgNPs demonstrated to have action in the cell wall and cellular membrane of many dermatophytes. The first step of AgNPs action is the adherence of AgNPs to the cell wall, followed by attacking their components causing weakness in ramification and preventing macroconidia development (Essghaier *et al.*, 2022). Al-Hamadani *et al.* (2017) found that the biosynthesis of AgNPs has many effects on the morphology and enzyme activity of *T. interdigitale* and *E. floccosum*. The hyphae of dermatophytes treated with AgNPs were swelled and lost integrity of membranes resulting to collapse the hyphae and wall disorganization. Another finding is that the keratinase activity of these dermatophytes was decreased after exposure to AgNPs (reduction of 47.41% for *E. floccosum* and 33.82% for *T. interdigitale*).

2.3.5 Antifungal activities of caspofungin nanoparticles

Few studies were found the antifungal effects of caspofungin combined with metallic nanoparticles (Carmo *et al.*, 2023). Synthetic golden nanoparticles with caspofungin (CAS-AuNPs) showed more antifungal action on *C. albicans* and non-albicans *Candida* (NAC) compared to caspofungin alone by causing damage in the fungal cell wall (Salehi *et al.*, 2021). Other thing, Caspofungin combined with zinc oxide nanoparticles enhanced antifungal action of caspofungin by reducing the MIC₅₀ of caspofungin from 15.47 to 10.34 µg/ml (Fayed *et al.*, 2021). The last study also showed a strange observation when the damage in the cell wall of *C. auris* after treated with caspofungin-ZnO NPs had

unpleasant results represented by increasing resistance to caspofungin through increasing chitin contents, overexpression of caspofungin target genes and resistant to fluconazole. The authors of this study explained this phenomenon by proposing that the morphological change caused by caspofungin-ZnO NPs results in *C. auris* aging faster with the inability to repair these changes. Loading of solid biomaterials surface with coated caspofungin combined with plasma polymerization of propionaldehyde (propanal) prevented the development of biofilm produced by *Candida* spp. on these surfaces and also prevented attachment of fungal cells on the surface of mammalian cells (Griesser *et al.*, 2015).

Chapter Three

Materials

and

Methods

3. Materials and methods

3.1 Materials

3.1.1 Apparatuses and equipment

The apparatus and instruments that were used in the experiments of the current study were illustrated in **tables 3-1** and **3-2**.

Table 3-1: Apparatuses of the study

No.	Apparatuses	Company	Country of origin
1	Autoclave	Hirayama	Japan
2	Bunsen burner	Jenway	German
3	Refrigerator	Vestal	Turkey
4	Incubator	Memmert	German
5	Shaking incubator	LaBTEch	Korea
6	Light microscope	Leica	German
7	Electronic balance	Kern abs	Korea
8	Hot Plate with magnetic stirrer	Panasonic	Japan
9	Laminar air flow hood	Olympus	Japan
10	Centrifuge	Hettich	German
11	Cooling centrifuge	LKB	Sweden
12	PCR thermal cycler	Bio-Rad	USA
13	Vortex mixer	Gemmy	U.S.A.

14	Haemocytometer	Marienfeld	German
15	Sonicator/ Ultra-sonic	Hwashin	Korea
16	Oven	Memmert	German
17	Water bath	Memmert	German
18	Electrophoresis power supply	Cleaver	Taiwan
19	Different sizes of micropipette	Dragon.med	Spain
20	Digital camera	Sony	Japan
21	pH meter	Jenwey	UK
22	Power supply	ESCO	USA
23	UV-transilluminator	U.V.P	USA
24	UV-visible spectrophotometer	Shimadzu	Japan
25	X-Ray Diffraction (XRD)	Shimadzu	Japan
26	Emission Scanning Electron Microscope (SEM)	TESCAN	Japan
27	FT-IR spectrophotometer	Shimadzu	Japan
28	Dynamic light scattering (DLS)	Shimadzu	Japan
29	Malvern Zeta sizer Nano ZS-90	Shimadzu	Japan

Table 3-2: Equipment of the study

No.	Equipment	Company	country of origin
1	Filter paper	Jiao Jie	China
2	Glass slides	ISOLAB	German
3	Microscope cover glass	Supertek	India
4	Steel inoculating loop	Loop Shandon	England
5	Forceps	Marienfeld	German
6	Gloves	Hi care	Thailand
7	Mask of face	YSK	Turkey
8	Tissues	Kardelen	Turkey
9	Different sizes of pyrex beakers	Marienfeld	German
10	Different sizes of pyrex conical flask	Marienfeld	German
11	Different sizes of pyrex cylinders	Marienfeld	German
12	Plastic petri dish	PlastLab	Lebanon
13	Screw vial	DARWELL	China
14	Glass tubes	DARWELL	China
15	Plastic microdilution plate (96 wells)	CITOTEST Labware Co. Ltd	China

16	Different sizes of eppendorf tubes	Merck	German
17	Sterilized cotton swabs	Mheco	China
18	Cotton	Wessam	Egypt
19	Aluminum foil	Deluxe	UAE
20	Micropipette tips	DARWELL	China
21	Plane tubes	Mheco	China
22	Dropper	Mheco	China
23	Thermometer	DARWELL	China
24	Scalpel	Zepf	German
25	Millipore filter	Mheco	China
26	Syringe (5ml)	Jiangsu	China

3.1.2. Chemical and biological materials

The chemical and biochemical materials used throughout the study are listed in the **table 3-3**.

Table 3-3: Chemical and biological materials

No.	Chemicals and biological Materials	Company	Country of Origin
1	Ethanol	Sentmenat	Spain
2	Potassium hydroxide	HiMedia	India
3	Caspofungin acetate	Sigma	German
4	Cefotaxime	LDP	Spain

5	Peptone	HiMedia	India
6	Agar Agar ,Type I	HiMedia	India
7	Glucose powder	SDI	Iraq
8	Sodium chloride solution 0.9%	FIPCO	Egypt
9	Cycloheximide /Actidione	CDH	India
10	Silver nitrate (AgNO ₃)	Merck	German
11	Trisodium citrate	HiMedia	India
12	Agarose	Promega	USA
13	Ethidium Bromide	Promega	USA
14	100-1500 bp DNA Ladder	Azma	Iran
15	Bromophenol blue	Promega	USA
16	PCR MasterMix	Azma	Iran
17	Primers	Bioneer comp.	Korea
18	TBE (Tris borate EDTA)	Promega	USA
19	Phosphate buffer saline (PBS)	PSI	Saudi Arabia
20	Glycerol	GCC	U.K
21	Potassium bromide	Promega	USA
22	Isopropanol	Sentmenat	Spain

3.1.3. Culture media

Cultured media that were already prepared were purchased as mention in the table 3-4.

Table 3-4: Already prepared culture media

No	Media	Manufacturing Company	country of origin
1	Sabouraud's Dextrose Agar (SDA)	HiMedia	India
2	Potato Dextrose Agar	Accumix®	Spin

3.1.4. Molecular requirements

Table 3-5: Primers sequences used for PCR.

Primer name	Sequences (5' _3')	Product size	Reference
ITS1	5'-TCCGTAGGTGAACCTGCGG-3	353 bp	Hsiao <i>et al.</i> , 2005
ITS2	5'-GCTGCGTTCTTCATCGATGC-3		

Table 3-6: PCR Master Mix components

Component	Concentration
Taq DNA polymerase	1U
dNTPs (dATP, dCTP, dTTP, dGTP)	400 mM for each one
Reaction Buffer	2X
MgCl ₂	83 mM
Deionized Nuclease –Free water	-

3.2 Methods

3.2.1 Media preparation

3.2.1.1. Sabouraud's glucose agar (SGA)

Sabouraud's glucose agar (SGA) was manually prepared by mixed glucose 20 g; agar 15 g, and peptone 10 g in a conical flask with 900 ml of distilled water. Mixture was shaken together until completely dissolved. Distilled water was added to the conical to complete the final volume of solution to one liter. Flask was sterilized by autoclave for 15 minutes at 121 °C under 15 Psi. After cooling to 45°C, cefotaxime powder (0.05 g/l) was added to media to block the growth of any contaminated bacteria. Sterilized media was poured in Petri dish or as a slant and kept in refrigerator at 4°C until use (Al-Janabi, 2011).

3.2.1.2 Sabouraud's glucose broth (SGB)

The same components of SGA in (3.2.1.1) were used for prepared Sabouraud's glucose broth (SGB), except diminution of agar. Components were shaken together until completely dissolved. Distilled water was added to the conical to complete the final volume of solution to one liter. Flask was sterilized by autoclave for 15 minutes at 121 °C under 15 Psi. After cooling to 45°C, cefotaxime powder (0.05 g/l) was added to media to block the growth of any contaminated bacteria. Sterilized media was poured in Petri dish or as a slant and kept in refrigerator at 4°C until use (Al-Janabi, 2011).

3.2.1.3 Sabouraud's dextrose agar (SDA)

Already prepared media of Sabouraud's dextrose agar (SDA) was used. The 65 g of media was dissolved in a conical flask with 900 ml of distilled water. Distilled water was added to the conical to complete the final volume of solution to one liter. Flask was sterilized by autoclave for 15 minutes at 121 °C under 15 Psi. After cooling to 45°C, cefotaxime powder (0.05 g/l) was added to media to block the growth of any contaminated bacteria. Sterilized media was

poured in Petri dish or as a slant and kept in refrigerator at 4°C until use (Al-Asadi, 2018).

3.2.1.4 Potato dextrose agar (PDA)

Already prepared media of potato dextrose agar (PDA) was used. The 39 g of media was dissolved in a conical flask with 900 ml of distilled water. Distilled water was added to the conical to complete the final volume of solution to one liter. Flask was sterilized by autoclave for 15 minutes at 121 °C under 15 Psi. After cooling to 45°C, cefotaxime powder (0.05 g/l) was added to media to block the growth of any contaminated bacteria. Sterilized media was poured in Petri dish or as a slant and kept in refrigerator at 4°C until use (Al-Asadi, 2018).

3.2.2. Preparation of reagents

3.2.2.1 Preparation of potassium hydroxide (20%) (KOH)

The solution of potassium hydroxide (KOH) was prepared by dissolving 20 g of KOH in 70 ml of sterile distilled water. Solution was completed to 100 ml by adding distilled water. After mixing, the solution was stored in screw vial at room temperature (Al-Asadi, 2018).

3.2.2.2. Rehydration of master mix

Two primers of *ITS* regions (*ITS1* and *ITS2*) were used in this study (**Table 3-5**). The lyophilized forms of primers were rehydration by adding a sterile deionized water to obtain a stock concentration of 100 pmol. This stock was diluted in free nuclease distilled water to obtain nearly 10 pmol. They were stored in the freezer until used in PCR amplification (Al-Asadi, 2018).

3.2.2.3 Preparation of caspofungin concentration

A stock solution of caspofungin (10 µg/ml) was prepared by dissolved 1mg of caspofungin acetate in 100 ml of sterilize distilled water (Al-Asadi, 2018).

3.2.3 Preparation of nanoparticles

3.2.3.1 Synthesis of silver nanoparticles

The solution of silver nanoparticles (AgNPs) was prepared as follows:

1. Powder 20 mg of silver nitrate was dissolved in 100 ml double-distilled water using a magnetic stirrer.
2. A 150 mg of trisodium citrate was added to the mixture. The temperature of the solution was adjusted to 80°C. The solution was vigorously stirred in this condition until the color of the solution turned to black. Temperature of the solution was cooled down to room temperature.
3. A 5 mL of concentrated glycerol was added while being vigorously stirred.
4. Solution was centrifuged at 12,000 RPM for 10 minutes and temperature of 20°C to get rid of the solvent and dried the precipitate (Salehi *et al.*, 2021).

3.2.3.2. Synthesis of caspofungin-silver nanoparticles

silver nanoparticles were used as a nano-core template to upload caspofungin on the surface. Caspofungin-silver nanoparticles (Ag@Cas NPs) were prepared by reducing silver nitrate with trisodium citrate in the presence of caspofungin as a stabilizer.

For the preparation of silver-caspofungin nanoparticles (Ag@Cas NPs):

1. Powder 20 mg of silver nitrate was dissolved in 100 ml double-distilled water using a magnetic stirrer.
2. A 150 mg of trisodium citrate was added to the mixture. The temperature of the solution was adjusted to 80°C. The solution was vigorously stirred in this condition until the color of the solution turned to black. Temperature of the solution was cooled down to room temperature.

3. A 5 mL of concentrated glycerol was added while being vigorously stirred.
4. A 70 mg of caspofungin acetate (CAS) was added in the solution of AgNPs at room temperature while being vigorously stirred in a magnetic stirrer for 5 minutes.
5. The mixture was sonicated using a probe-type ultrasonic (400 W, 50% power, 50% cycle) for 10 minutes to form Ag@Cas NPs.
6. Solution was centrifuged at 12.000 RPM for 10 minutes and temperature of 20°C to get rid of the solvent and dried the precipitate (Salehi *et al.*, 2021).

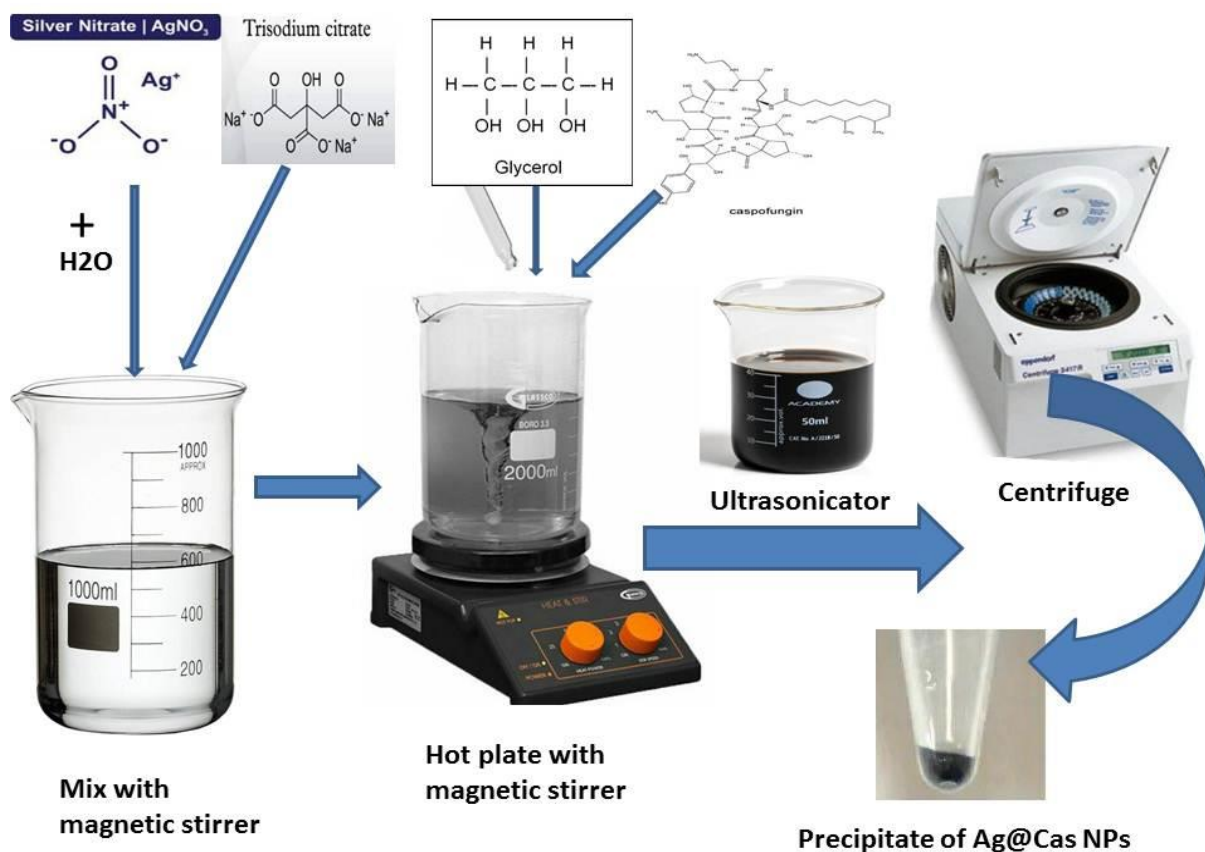


Figure 3.1: illustration of synthesis of Ag@Cas NPs method used used as a nano-core template to upload caspofungin on the surface by reducing silver nitrate with trisodium citrate in the presence of caspofungin.

3.2.3.3 Synthesis of modified caspofungin-silver nanoparticles

Another structure of AgNPs was prepared direct the synthesis of modified by removing reducing agent trisodium citrate. This synthesis AgNPs was also mixed with CAS to form modified caspofungin-silver nanoparticles (modified Ag@Cas NPs) as in the following steps:

1. A 5 mg of silver nitrate was dissolved in 20 ml of double-distilled water using a magnetic stirrer to be solution no. 1.
2. A 5 mg of caspofungin acetate was dissolved in 20 ml of double- distilled water to be a solution no. 2.
3. Solution 2 was mixed with solution 1 gradually by dropper with vigorously stirred.
4. Mixture was left for 30 min at temperature room, then increased temperature to 30°C for 30 min, and 40°C for 30min, until the colour of the solution turned to black.
5. Solution was centrifuged at 12.000 RPM for 10 minutes and temperature of 20°C to get rid of the solvent and dried the precipitate (Salehi *et al.*, 2021).

3.2.4 Characterization of synthesized nanoparticles

Several techniques, including UV–visible Spectrophotometer, Zeta potential, XRD, FT-IR and SEM were used for characterization of nanoparticle compounds.

3.2.4.1 Ultraviolet-visible- (UV–vis) spectroscopy analysis

UV-spectroscopy is of simple and an easy method for characterizing nanoparticles and it is commonly used to confirm the presence of nanoparticles in a liquid (Qureshi, 2013). The UV- visible absorbance spectral analysis of

nanoparticles were recorded by using UV-vis spectrophotometer in a 10 mm path length quartz cuvette (Malik *et al.*, 2021) within the range of 200-1200 nm.

3.2.4.2 Scanning electron microscopy (SEM)

Scanning electron microscope (SEM) is a technique mainly used to detect the crystalline structure or morphological characteristics of prepared nanoparticles with the ability to determine the particle size of the nanocomposites (Qureshi, 2013). A small drop of the nanoparticles was placed on a carbon coated copper grid, left to dry at room temperature, and then exposed to device SEM (Sabir *et al.*, 2022).

3.2.4.3 Determination of particle size distribution

Dynamic light scattering (DLS) is used to determine the hydrodynamic particle size distribution of the samples with assessment by using a Zetasizer Nano instrument. The zeta potential indicates the charge acquired by a particulate system on its suspension in aqueous medium. The surface charge and size were performed by DLS (Gómez-Sequeda *et al.*, 2017). Malvern Zetasizers® was used a laser with 4 mW He\Ne laser of 633 nm wavelength. DLS was also supplied in the same instrument with other wavelengths e.g 532 nm. Square cuvettes that is made of scratch-free glass and those of optically translucent disposable plastic were used. The same instrument was supplemented with a plastic cuvettes with inbuilt electrodes capable of both DLS and ZP measurements. The tested sample was prepared in characterizes of cleaning, homogeneous, transparent, and without any precipitation. Sample was prepared at minimal volume with at least 1–2 ml to get high quality data (Bhattacharjee, 2016).

3.2.4.4 Fourier transform infrared spectroscopy FT-IR

Fourier transform infrared spectroscopy (FT-IR) is used to identify the chemical bonds, structure and functional groups of biomolecules of the prepared NPs (Al-Janabi and Bashi, 2022; Essghaier *et al.*, 2022; Kumar, 2006). The nano solution was dried and mixed with potassium bromide at ratio of 1: 100. Mixture was displayed using the FT-IR instrument in a frequency range of 400 to 4000 cm⁻¹ (Nayak *et al.*, 2020; Kumar, 2006).

3.2.4.5 X-Ray diffraction (XRD)

The mean crystallite size of nanoparticles was quantitatively determined from XRD data depending on the crystal size using Scherrer equation (Mehta *et al.*, 2017):

$$D = k\lambda/\beta\cos\theta$$

Whereas: D: Average crystallite size, K=0.9: The shape factor, λ : The X-ray wavelength (in nm), θ : The Bragg diffraction angle $38.164/2$

β : The full width at half maximum (FWHM) of the intense peak (in radians).

The crystallinity and phase were analyzed using powder of nanoparticles on a glass slide at an angle 2θ and with a temperature range of 20- 80 ° C.

3.2.5 Isolation of dermatophytes:

After clinical examination of 100 patients with suspected dermatophytoses, dermatophytes were successfully isolated from seven patients while admitted to Al-Imam Al-Hussein Medical City Hospital in Karbala in Iraq from August to November 2023. Patients included 3 males (5-25 years) and 4 females (19-40 years). Dermatophytes were isolated by scraping infected lesion of skin and collected hair specimens from involved patients. Dermatophytoses were preliminary diagnosed based on clinical

features noticed by dermatologists of consultation department of the hospital. Edge of lesion was the location of scraping collection after cleaned with 70% ethyl alcohol. Two specimens from the same lesion was collected. The first one was directly examined under the microscope with 20% KOH looking for fungal elements (conidia and hypha). The second specimen was cultured on SDA and incubated at 30°C for up to 2 weeks. Morphological characters of grown fungi were microscopically examined to identify the shape of macroconidia, microconidia, and hypha arrangement (Rippon, 1988). Characters of colonies, including texture, and color of front and reverse view of colonies were also determined.

3.2.6 Genotyping detection

Molecular approaches of DNA extraction, PCR reaction and gene sequences were used to final diagnosis of dermatophytes.

3.2.6.1 DNA extraction

DNA of dermatophytes was extracted by boiling method that was described by Galliano *et al.*, (2021) with some modification. A colony of two weeks culture of dermatophyte on SDA were boiled in 2 ml PBS for 10 min. Mixture was vortexed and boiled for another 10 min and then centrifuged at 13000 g for 5 min at 25 °C. A 250 µl of supernatant were added to an equal amount of isopropanol, and incubated at -4 °C for 30 min. After centrifugation at 13,000 g for 2 min, the pellet was washed with 70% ethanol, and centrifuged at 13,000 g for 5 min. Solution was dried and suspended in 200 µl of TBE buffer.

3.2.6.2 PCR amplification

The PCR amplification was used for complete diagnosis of isolated dermatophytes. PCR mixture was prepared in eppendorf tubes to be 25 µl as a

final volume. This volume was composed of 12.5 µl of PCR Master Mix (1x), 5 µl of template DNA, 1 µl of each primer, and 5.5 µl of nuclease free water. Tube was mixed briefly via vortex then placed in thermocycler polymerase chain reaction (PCR). The program of PCR was illustrated in the **table 3-7**.

Table 3-7: The PCR condition for amplification of ITS regions

Primer	PCR step	Temperature	Time	Repeat	Reference
<i>ITS1</i> and <i>ITS2</i>	Initiation	95 °C	7 min	1	Hsiao <i>et al.</i> , (2005) with some modification
	Denaturation	95 °C	1 min	35 cycles	
	Annealing	62 °C	1 min	1	
	Extension	72 °C	1 min	1	
	Final extension	72 °C	10 min	1	

3.2.6.3 Agarose gel preparation

Amplified products of PCR were identified by gel electrophoresis. Quality of the extracted DNA was identified by using agarose gel, which was prepared in 1% concentration by dissolving 1g of agarose powder in 100 ml of 1X TBE buffer in 250 ml conical flask. Agarose suspension was melted until homogenized by using microwave for 1 min. After cooling of gel to 60° C, 0.5 µg/ml of ethidium bromide was added. Cooled agarose was poured on electrophoresis tray containing a plastic comb after the fin, which removed after solidification of agarose to obtain wells (Morovat *et al.*, 2009).

3.2.6.4 Electrophoresis method:

The prepared agarose was submerged in the electrophoresis tank filled with 1 X TBE buffer. A 3.5 µl of each DNA sample was mixed with 1.5 µl of loading dye (Bromophenol blue) and loaded in each well within agarose. A 100 bp of DNA ladder in amount of 10 µl was also loaded in the middle well of the agarose electrophoresis gel. A special lid was used to closed the electrophoresis tank and powered on with a 85 V and 170 A for 30 min. Gene band in the final product was examined under short wavelength of UV by gel documentation instrument (Green and Sambrook, 2001).

3.2.6.5 Sequencing of *ITS* regions

PCR products of 7 forward and reverse *ITS* regions samples of dermatophytes were stored at – 20 °C, then the nucleotides sequence of gene were carried out by sending the samples and primer to sequence company (Bioneer, Korea). After the results arrived, homology search was conducted using Basic Local Alignment Search Tool (BLAST) program which is available at the National Center Biotechnology Information (NCBI) online to know the close strain of dermatophytes.

3.2.7 Antifungal susceptibility assay of prepared nanoparticle

materials:

A disc diffusion method was used to evaluate antifungal effects of prepared nanoparticle materials against dermatophytes based on method described by Nweze *et al.* (2010). The isolated dermatophytes were regrown by cultured on SGA and incubated at 30° C for one week. Hemocytometer technique was used to prepared standard cell number of dermatophytes. This adjustment cell number was prepared by suspension a small amount of dermatophyte cells by loop from grown colony and suspended in sterilized

normal saline. Shaking by vortex was used to fragmentation of fungal cells in the mixture. A drop from such suspension was loaded into the hemocytometer to check the number of fungal elements. The fungal suspension was adjusted to be approximately $1.5-2 \times 10^6$ cell/ml³ which was considered a standard concentration for all isolated dermatophytes. A 100 µl of adjusted count was inoculated on a plate with SGA by spreading with swab. A number of discs that have 6 mm in diameter were prepared from filtered paper. The discs were impregnated in solution containing different concentrations of prepared nanoparticle materials (500, 250, 125 and 62.5)mg/ml. Such discs were loaded on the inoculated plate by sterilized forceps. Plates were incubated for four days at 30 °C. A discs with either caspofungin acetate (0.001 mg/ml) or AgNPs were used as a positive controls. The zone of inhibition was measured in mm around effective disc.

3.2.8 Minimum inhibitory concentration (MIC) of prepared nanoparticle materials:

The MIC of prepared nanoparticles materials in dermatophytes was determined based on the broth dilution method mentioned by **CLSI-M38-A2 (2008)**. All isolated fungi were sub-cultured on SGA at 30° C for 1-3 weeks for activation. Adjusted $1.5-2 \times 10^6$ cell/ml³ of dermatophytic cells by hemocytometer was used. A double-serial concentrations of prepared nanoparticle materials were prepared from a stock concentration (100 mg/ml) (50, 25, 12.5, 6.25, 3.125, 1.562 mg/ml). A plastic microdilution plates (96 wells) were used to determine the MIC value. Each well of the plates received 100 µl of SGB, 50 µl of standard count of each fungal suspension, and 50 µl of specific concentration of prepared nanoparticle materials. Two controls were used within a single microdilution plate. The positive control included SGB with AgNPs only and SGB with CAS. The negative controls were SGB with fungi only and SGB with distilled water. Inoculated plate was covered with a

sterilized aluminum foil for preventing plate contents from dryness and contaminated during incubation periods. The plate was incubated at 30° C for 72 hours. The presence or absence of fungal growth based on visual determine was considered as a results.

3.2.9 Statistical analysis:

All data of all experiments were expressed as mean \pm SD. Statistical analysis of the data was performed using of one way of analysis of variance (ANOVA) through the application of Excel of Windows 10. The minimum level of (P) value was < 0.05 concerts as significant level.

CHAPTER FOUR

RESULTS

4. Results:

4.1 Synthesis and characterization of caspofungin-silver nanoparticles

4.1.1 Ultraviolet-visible- (UV-vis) spectroscopy analysis

The properties of optical absorption of the prepared samples were determined by Ultraviolet-visible-Near Infrared spectra (UV-vis-NIR). As shown in (Figure 4.1), Caspofungin had a typical absorption spectrum with absorption bands centered at 200 nm. Meanwhile, the characteristic absorption peak of Ag@Cas NPs absorbed strongly from mean \pm 350-900 nm. The aberrance of the characteristic absorption peak of caspofungin near 200 nm in the spectrum of Ag@Cas NPs well demonstrated the uploading of caspofungin on the AgNPs and formation of Ag@Cas nanoparticles.

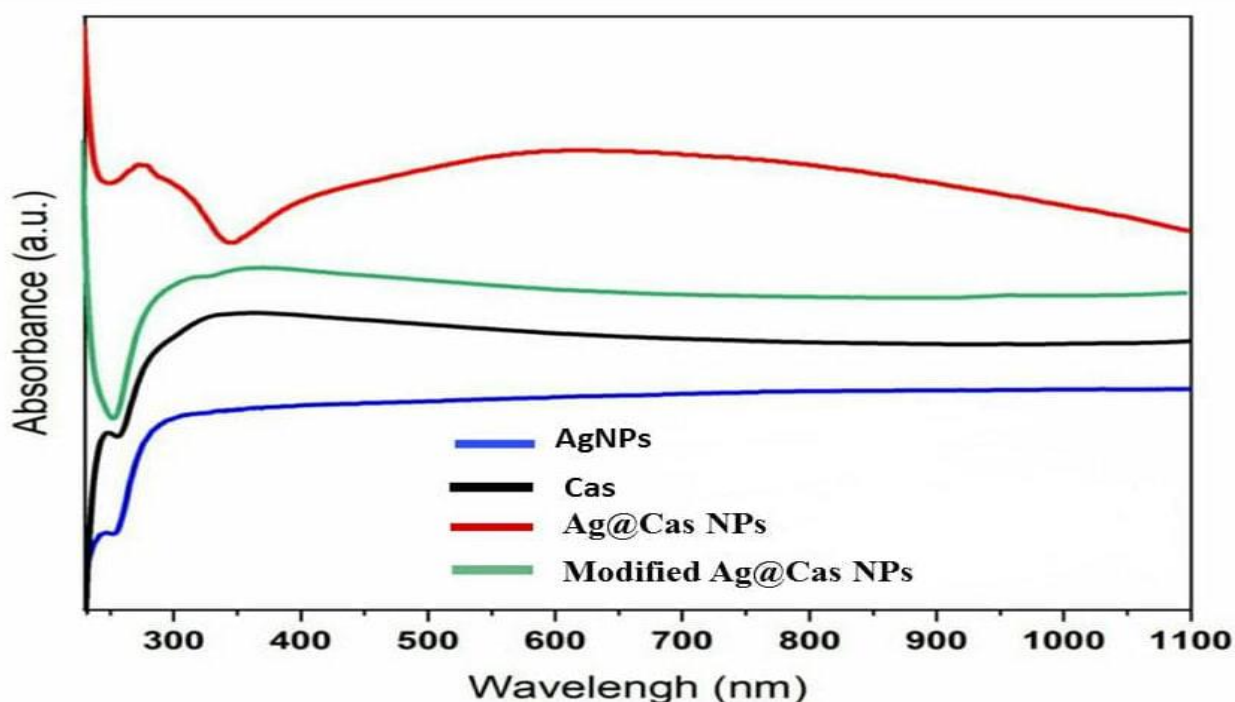


Figure 4.1: UV-vis-NIR spectra of AgNPs (blue line), Ag@Cas NPs (red line), modified Ag@Cas NPs (green line), caspofungin (Cas.) (black line).

4.1.2 Scanning electron microscopy (SEM)

The characters of morphology and structure of the prepared nanoparticles were identified by using scanning electron microscopy (SEM). The SEM images showed that the synthesized AgNPs exhibited a smoothly spherical shape (Figure 4.2 a). After *in situ* growing caspofungin on the surface of AgNPs, a sphere-like structure is maintained well with an enlarged diameter, revealing the existence of the caspofungin coating layer. The resulting Ag@Cas NPs nanocomposites displayed a spherical external layer around the sphere AgNPs, suggesting, a formation of core-shell Ag@Cas nanostructures (Figure 4.2 b). A direct synthesis procedure of modified Ag@Cas NPs structure without using any reducing agent, exhibited a larger size of Ag@Cas NPs micromolecules from mean $\pm 0.3 - 0.5 \mu\text{m}$ (Figure 4.2 c).

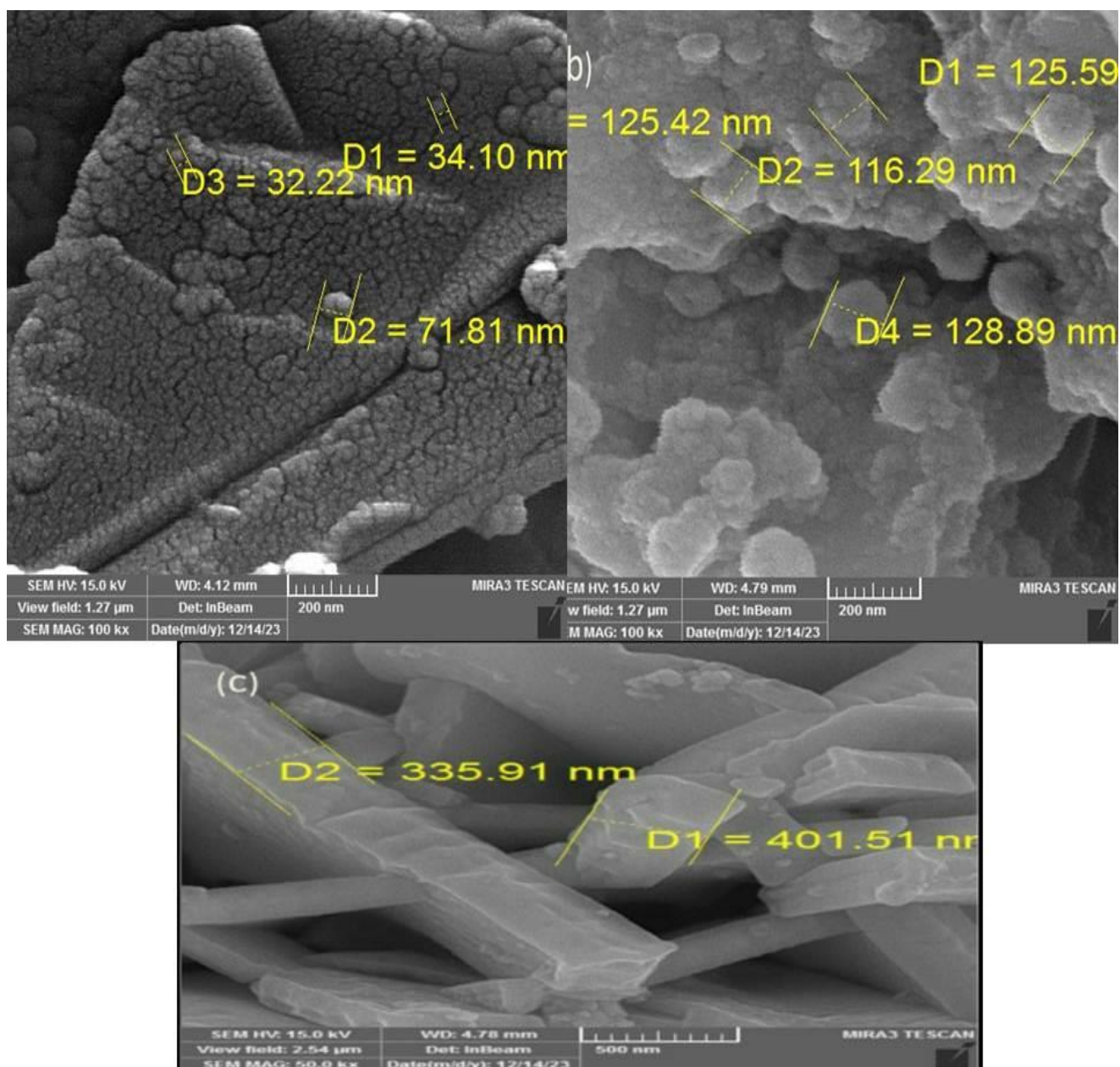


Figure 4.2: SEM images of (a) AgNPs, (b) Ag@Cas NPs, (c) modified Ag@Cas NPs

The distinct particle sizes of the as-prepared nanoparticles were calculated from SEM images as shown in Figure 4.3. The average particle sizes of synthesized AgNPs were distributed from mean \pm 20-100 nm, with an increase in the particle sizes after adding the caspofungin drug. The particle size distribution increased from mean \pm 60-150 nm, which is attributed to the uploading of the caspofungin molecules on the surface of silver nanoparticles.

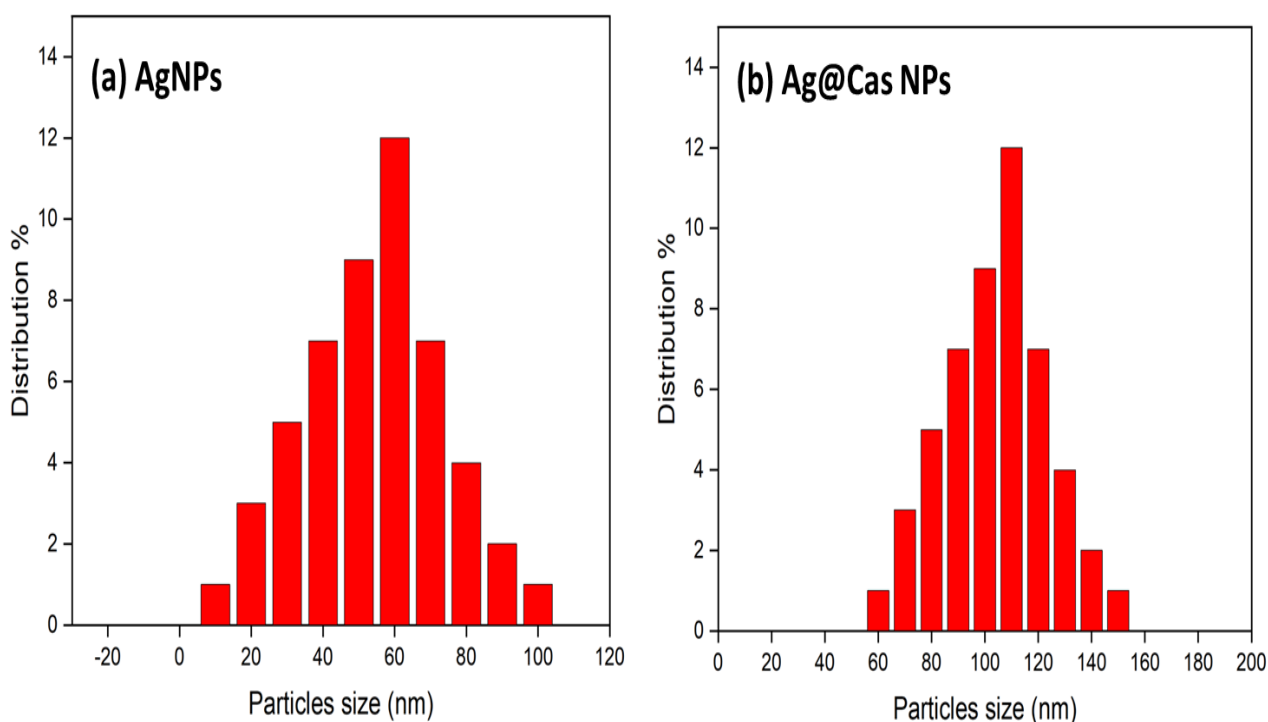


Figure 4.3: Sizes distribution calculated from SEM images of (a) AgNPs, (b) Ag@Cas NPs.

4.1.3 Determination of particle size distribution

The particle sizes of the prepared nanomaterials were examined by dynamic laser scattering (DLS), and they appear to be greater than those measured by SEM. The diameters of AgNPs were determined in mean \pm 100 nm and they increase in the average size from mean \pm 100 nm to mean \pm 250 nm after fusing with the caspofungin (Figure 4.4). This analysis demonstrating the successful formulation of Ag@Cas NPs nanocomposites. On the other hand, modified Ag@Cas NPs showed a further increase in the particle size up to 400 nm. These results well confirm the incorporation of caspofungin on the surface of the silver nanoparticles.

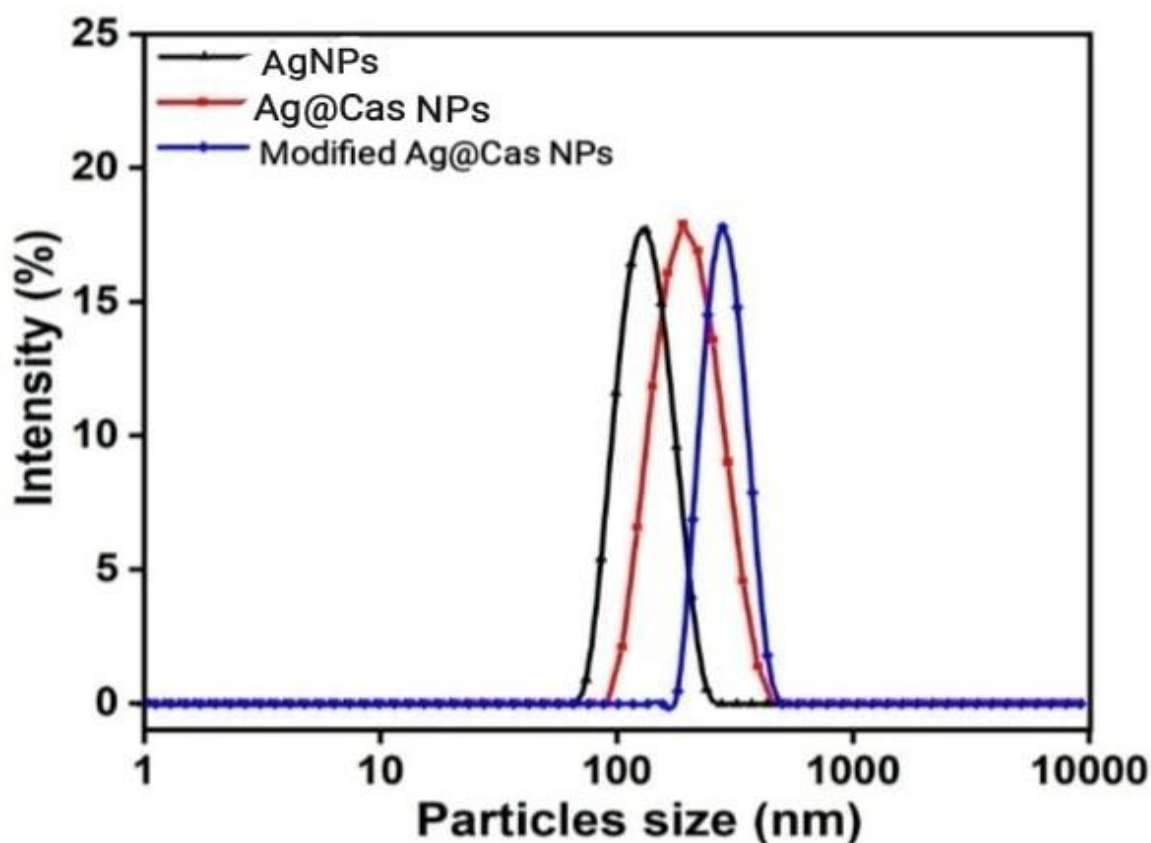


Figure 4.4: DLS results of AgNPs (black line), Ag@Cas NPs (red line), modified Ag@Cas NPs (blue line).

Moreover, the corresponding Zeta-potentials of the prepared nanoparticles were assessed by formulation with Ag to get surface charges of Ag@Cas NPs (Figure 4.5). The Zeta-potentials was transformed from -14.2 to -48 mV. The negative shift is an indicator to the development of negatively charged carboxyl and hydroxyl ions which are dominant negative functional groups in the caspofungin groups. The results further approve the successful presence of caspofungin on the surface of silver nanoparticles.

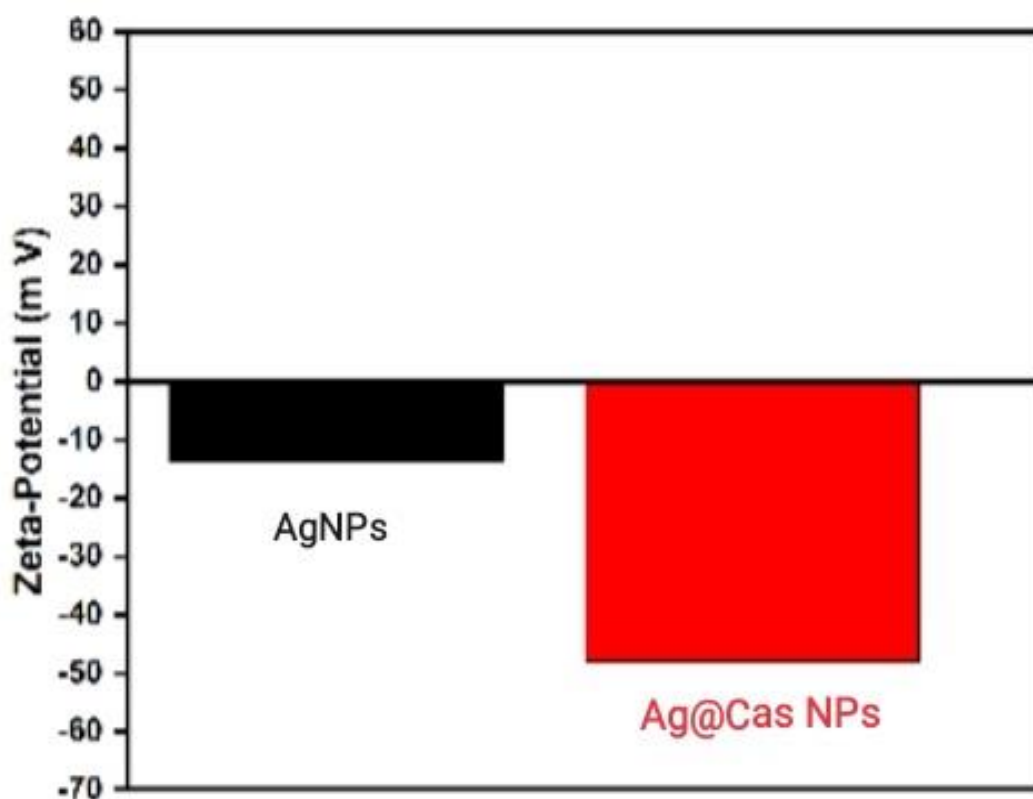


Figure 4.5: Zeta-potentials of AgNPs (black), Ag@Cas NPs (red).

4.1.4 Fourier transform infrared spectroscopy FT-IR

Moreover, to confirm the success of uploading caspofungin on the surface of silver nanoparticles, FT-IR analysis was taken into consideration, as shown in (Figure 4. 6). The FT-IR spectrum of Ag@Cas NPs showed a broad strong peak at 3361 cm^{-1} which can be attributed to both N-H and O-H stretching vibration of caspofungin. The sharp peaks at 2935 cm^{-1} and 2883 cm^{-1} revealed the vibration of aromatic and aliphatic C-H stretching, of caspofungin, respectively. The bands at 1647 cm^{-1} and 1591 cm^{-1} are attributed to C=O of the acid and amide groups of caspofungin, respectively. The peaks around 1380 cm^{-1} correspond to the C = C and C-N stretching. The peak at 1043 cm^{-1} corresponds to C-O stretching. The peaks at 852 cm^{-1} , 696 cm^{-1} , and 569 cm^{-1} were attributed to the attachment of silver with the -OH, C-H, and -C=O groups. These results prove that caspofungin was loaded on the silver nanoparticles surface and the formulation of Ag@Cas NPs.

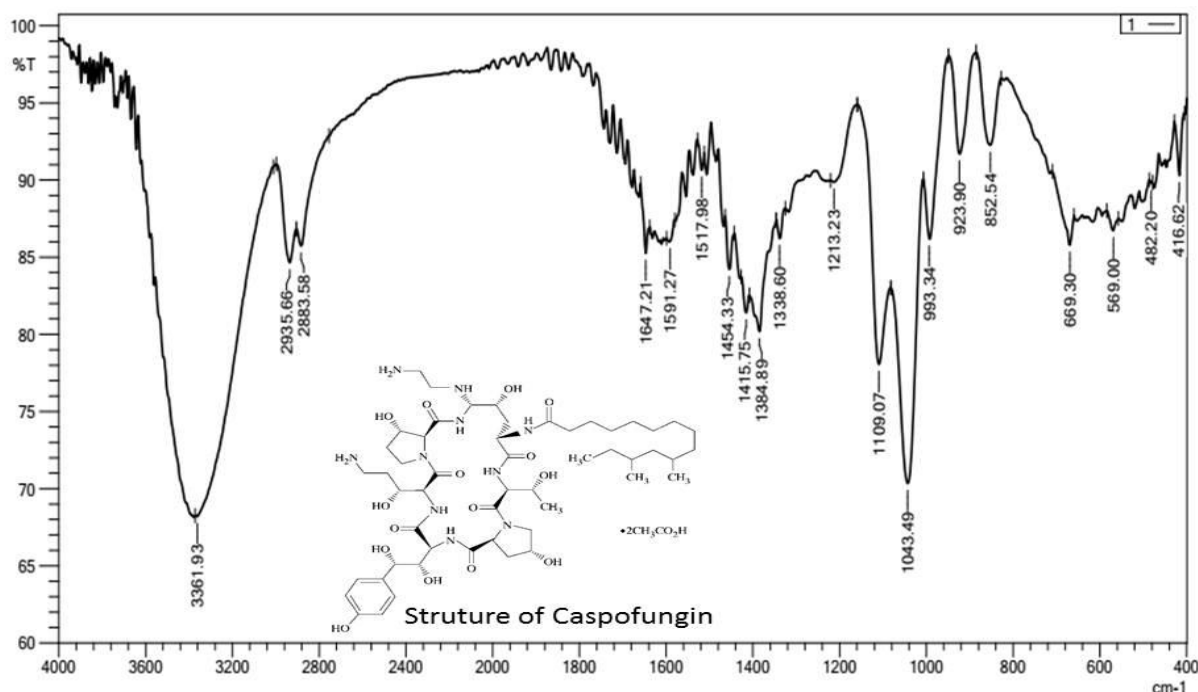


Figure 4.6: FT-IR Spectrum of synthesized Ag@Cas NPs, with structure of caspofungin.

4.1.5 X-Ray diffraction (XRD)

The crystallinity of the as-prepared Ag@Cas NPs was studied by X-ray diffraction (XRD) pattern. As displayed in (Figure 4.7), there are no obvious sharp peaks seen in the XRD pattern, confirming that the as-prepared nanoparticles are less crystalline and more amorphous in nature which due to the organic soft nature of caspofungin. The peaks at 27°, 33°, and 46 ° are attributed to the silver nanoparticles. These results completely agreed with SEM images, suggesting the formation of spherical hydrogel and uploading of caspofungin on the AgNPs.

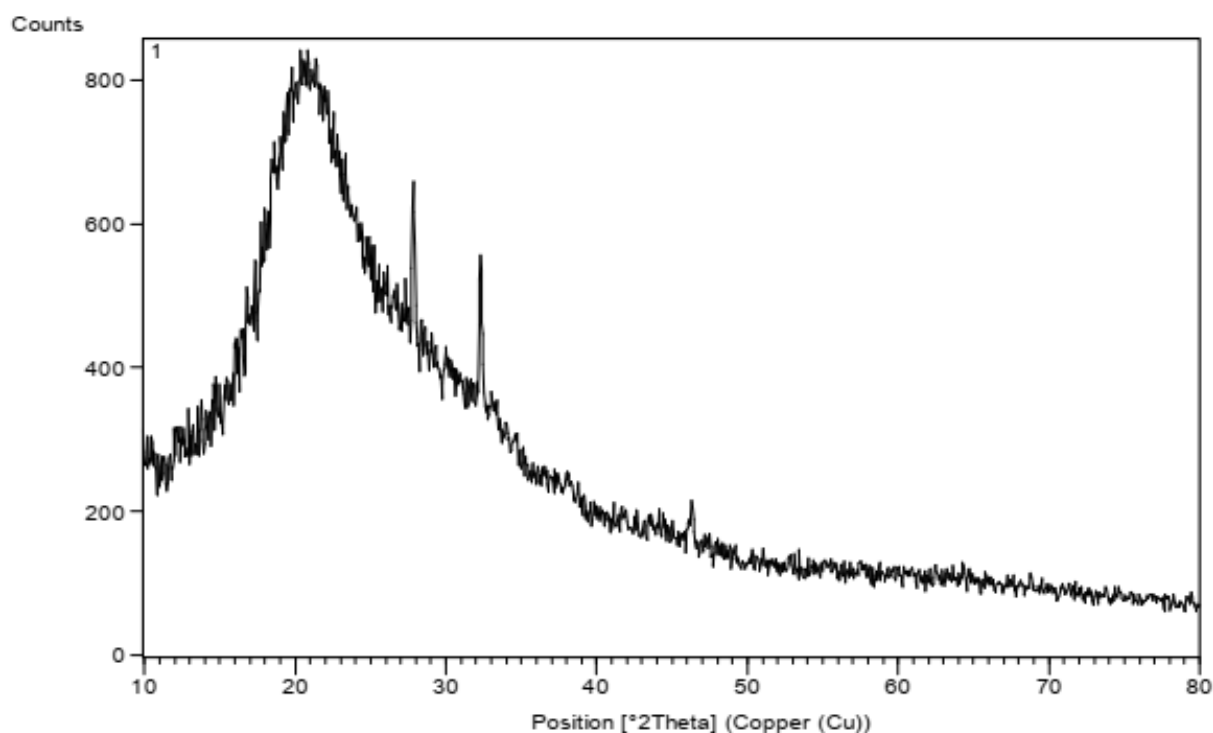


Figure 4.7: XRD pattern of Ag@Cas NPs.

4.2 Identification of dermatophytoses and dermatophytes

Dermatophytoses were clinically diagnosed in 100 patients during visiting dermatological consultation of the AL-Hussein Medical City. Dermatophytes were successfully isolated from 7 patients (3 males and 4 females) with different types of tinea (Table 4-1). The age of dermatophytoses patients was

ranged between 5 and 40 years. Three types of tinea, including tinea capitis, tinea pedis, and tinea barbae were separately diagnosed in males, while females had tinea corporis (2 cases) and tinea cruris (2 cases) (Table 4-1).

Three species of *Microsporum* genus (*M. canis*, *M. ferrugineum* and *M. gypseum*) and four of *Trichophyton* (isolate one of *T. mentagrophytes* (*T. mentagrophytes-1*), isolate two of *T. mentagrophytes* (*T. mentagrophytes-2*), isolate one of *T. indotineae* (*T. indotineae-1*), and isolate two of *T. indotineae* (*T. indotineae-2*) were diagnosed based on morphological characters and molecular characters. Genetic bands of the *ITS1* & *ITS 2* regions by PCR for all isolates were clearly identified (Figure 4.8).

Table 4-1: Dermatophytoses with species of dermatophytes

Gender	Dermatophytoses	Patients No.	Age mean (years)	Fungal isolation
Males	Tinea capitis	1	5	<i>M. canis</i>
	Tinea pedis	1	25	<i>T. mentagrophytes-1</i>
	Tinea barbae	1	19	<i>M. ferrugineum</i>
Females	Tinea cruris	2	25	<i>M. gypseum</i> <i>T. indotineae-1</i>
	Tinea corporis	2	15	<i>T. indotineae-2</i> <i>T. mentagrophytes-2</i>



Figure 4.8: PCR products of *ITS 1* and *ITS 2* regions of 7 strains of dermatophytes with Ladder DNA at the middle.

1. *M. canis*, 2. *T. mentagrophytes*-1, 3. *M. ferrugineum*, 4. *T. indotineae*-1,
5. *T. indotineae*-2, 6. *T. mentagrophytes*-2, 7. *M. gypseum*

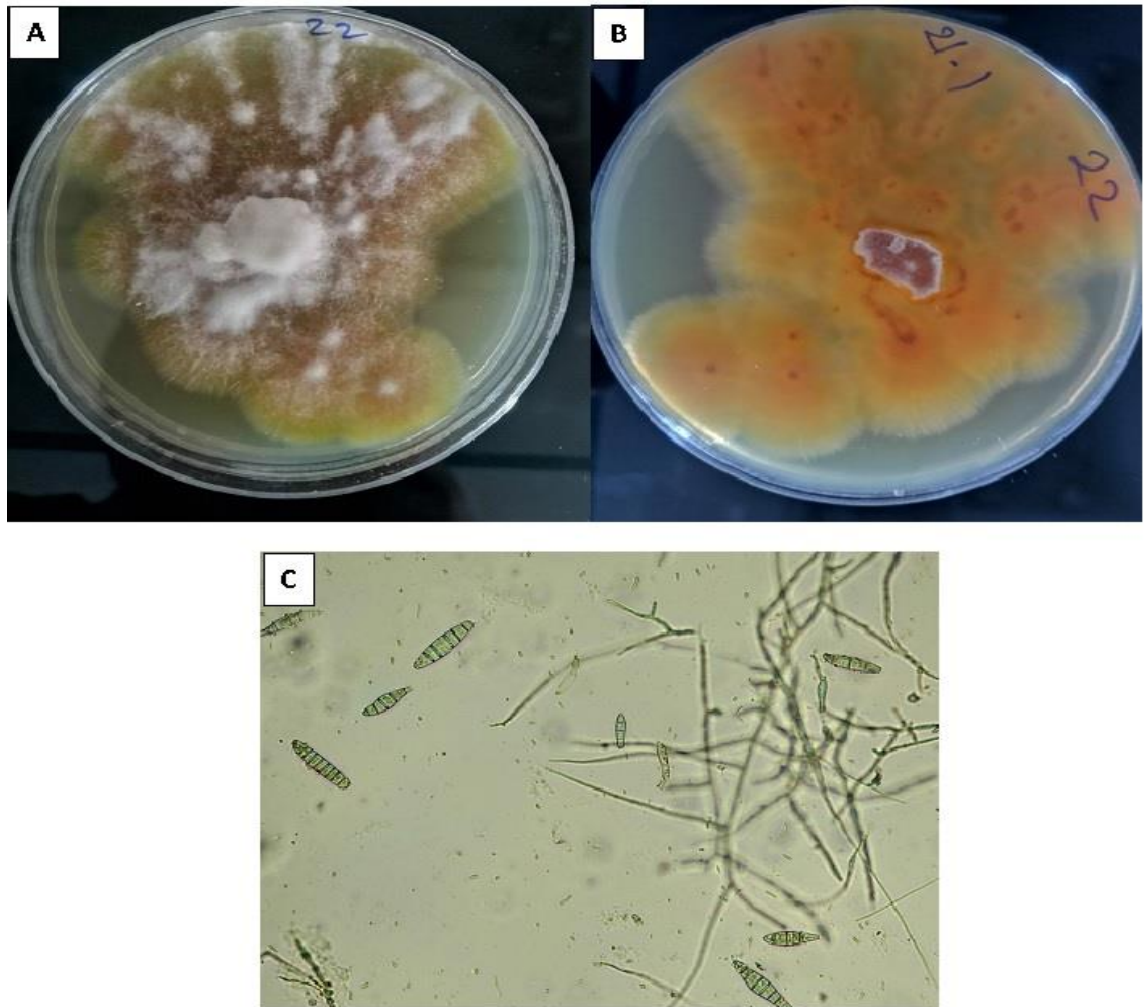


Figure 4.9: Colony of *M. canis*

A: Colony in front view, **B:** Colony in reverse view, **C:** Microscopic view

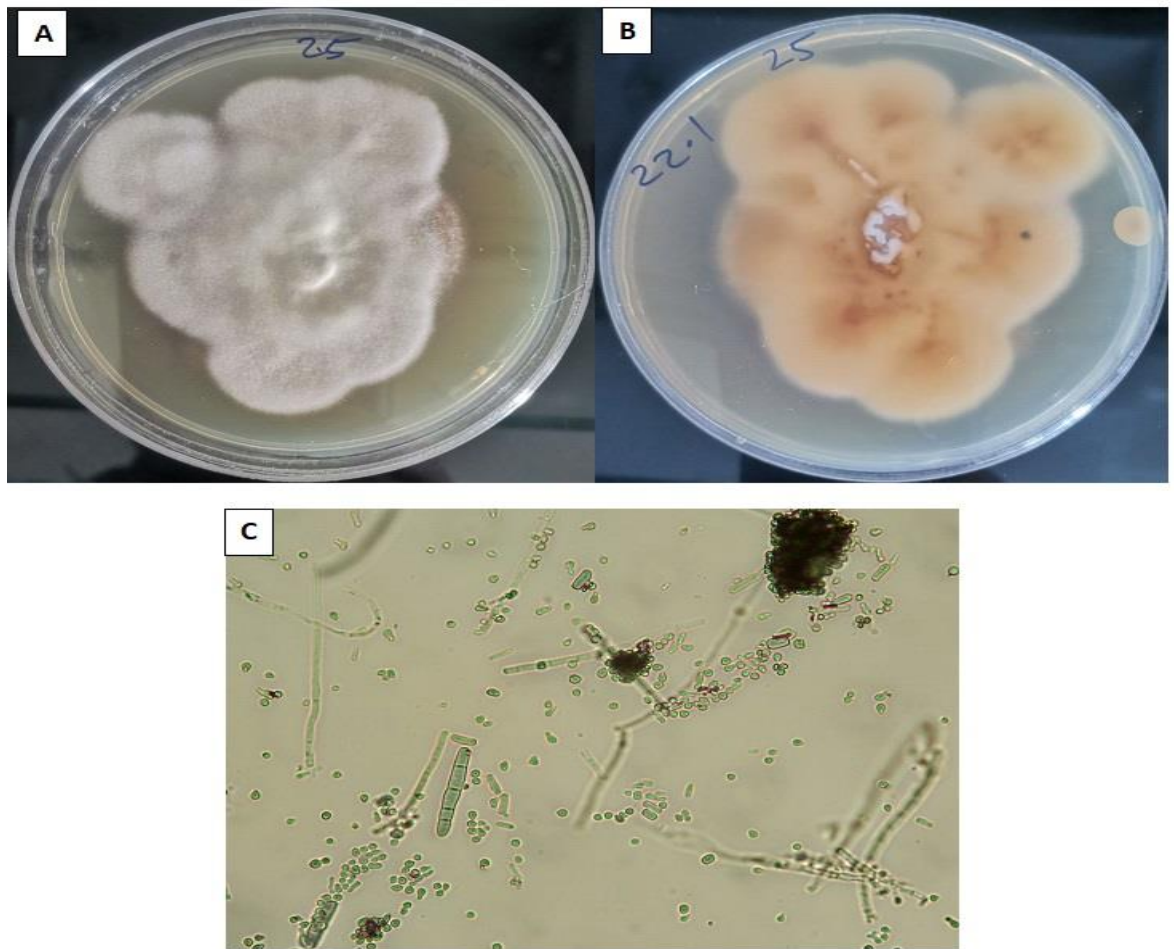


Figure 4.10: Colony of *T. mentagrophytes-1*

A: Colony in front view, **B:** Colony in reverse view, **C:** Microscopic view

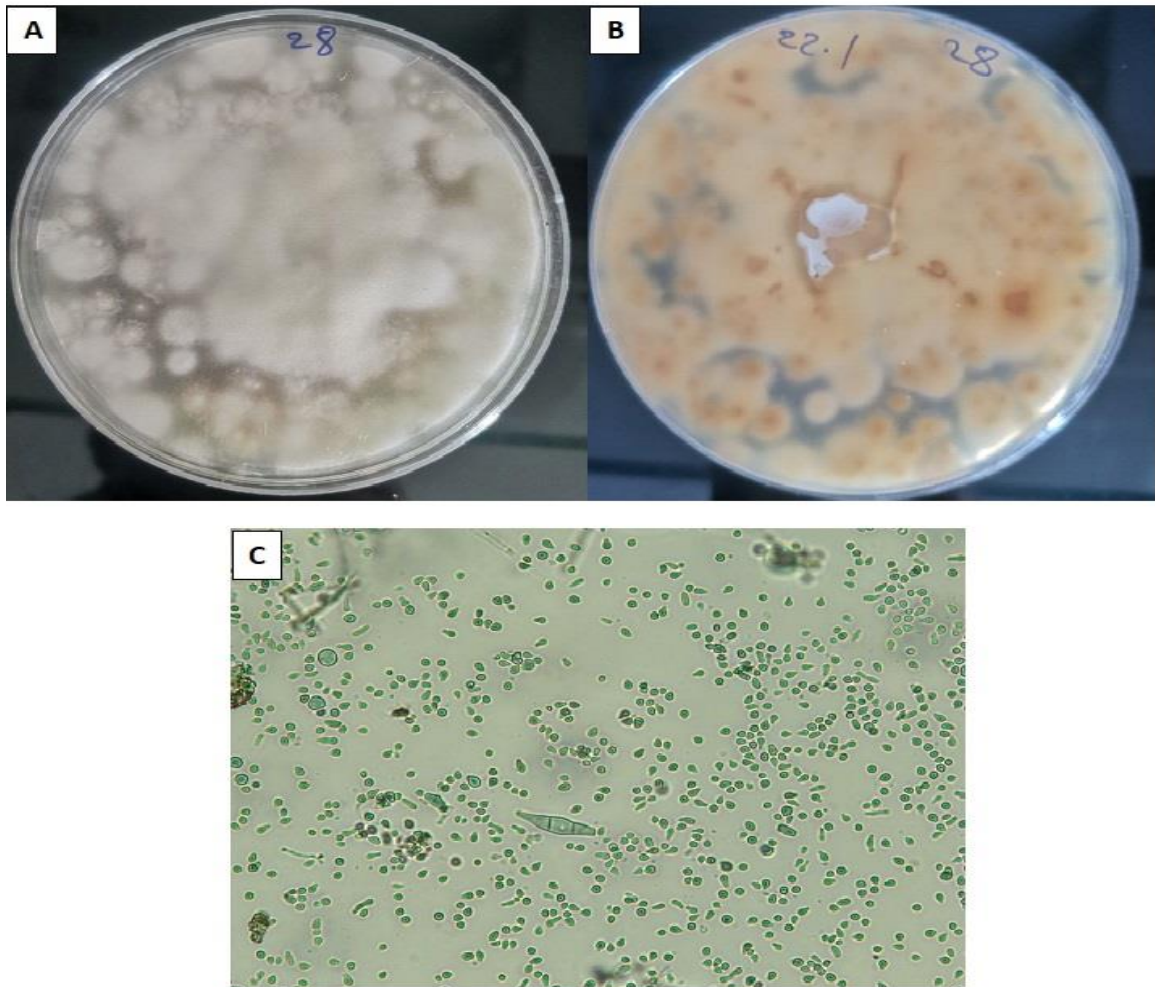


Figure 4.11: Colony of *M. ferrugineum*

A: Colony in front view, **B:** Colony in reverse view, **C:** Microscopic view

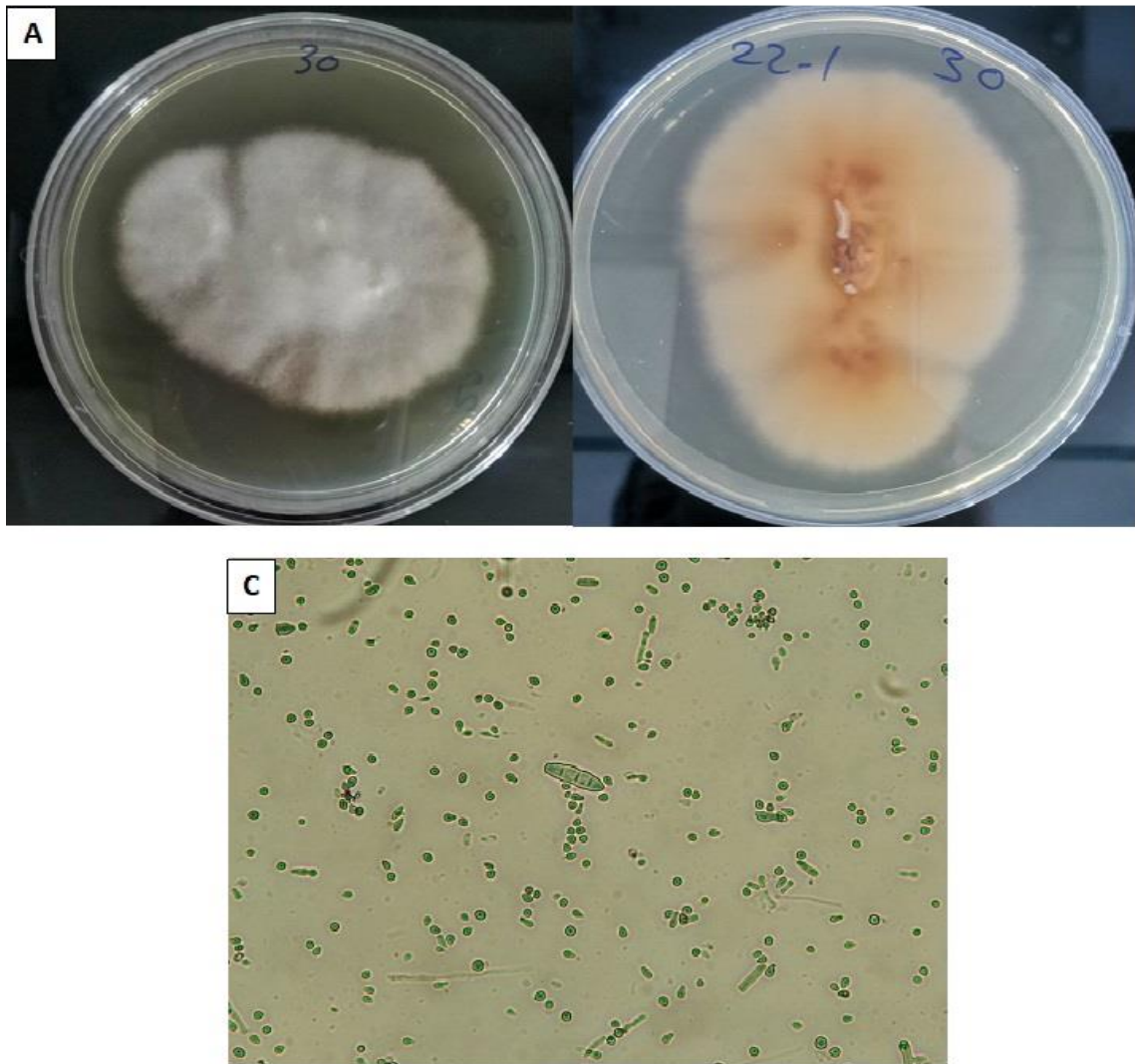


Figure 4.12: Colony of *T. indotineae-1*

A: Colony in front view, **B:** Colony in reverse view, **C:** Microscopic view

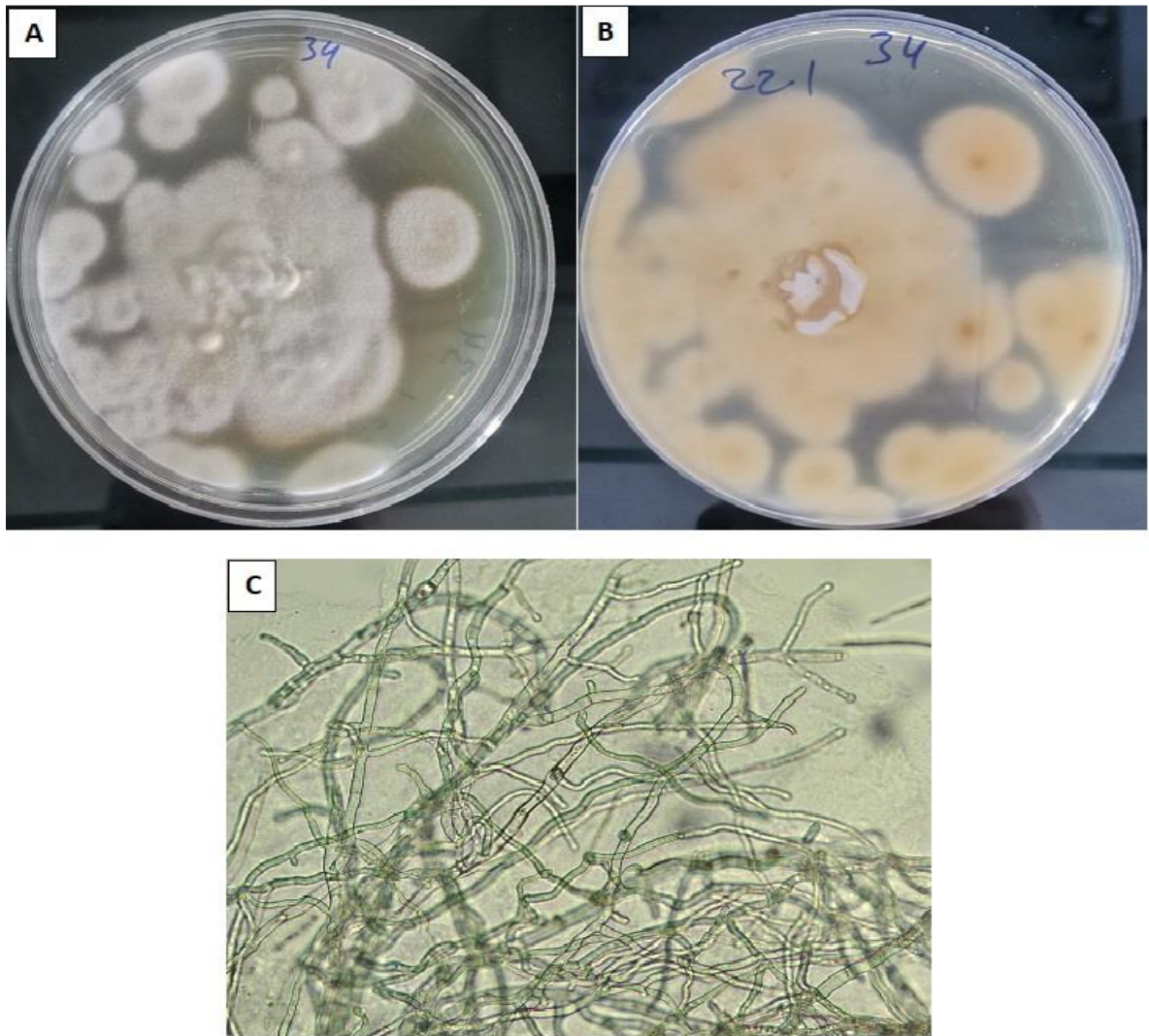


Figure 4.13: Colony of *T. indotineae-2*

A: Colony in front view, **B:** Colony in reverse view, **C:** Microscopic view

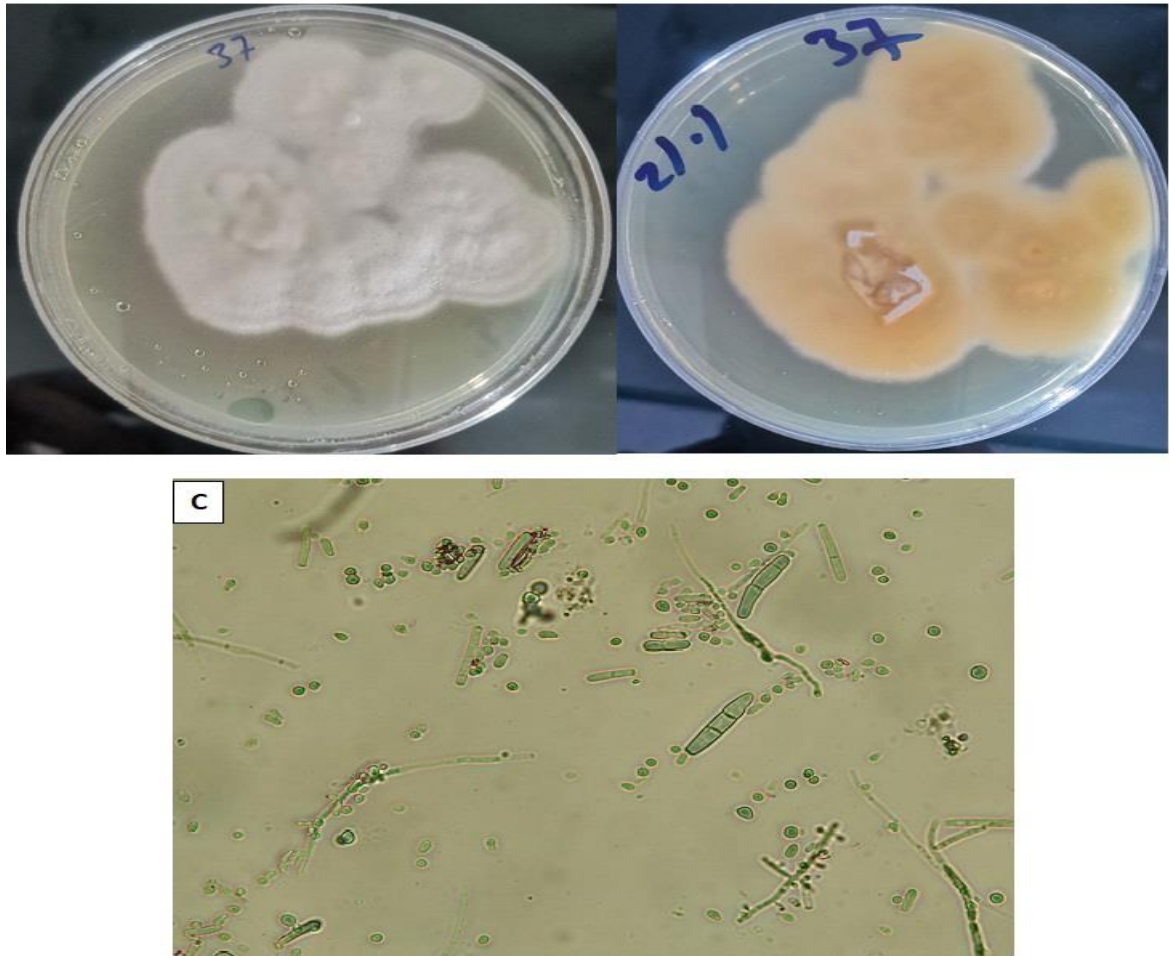


Figure 4.14: Colony of *T. mentagrophytes-2*

A: Colony in front view, **B:** Colony in reverse view, **C:** Microscopic view

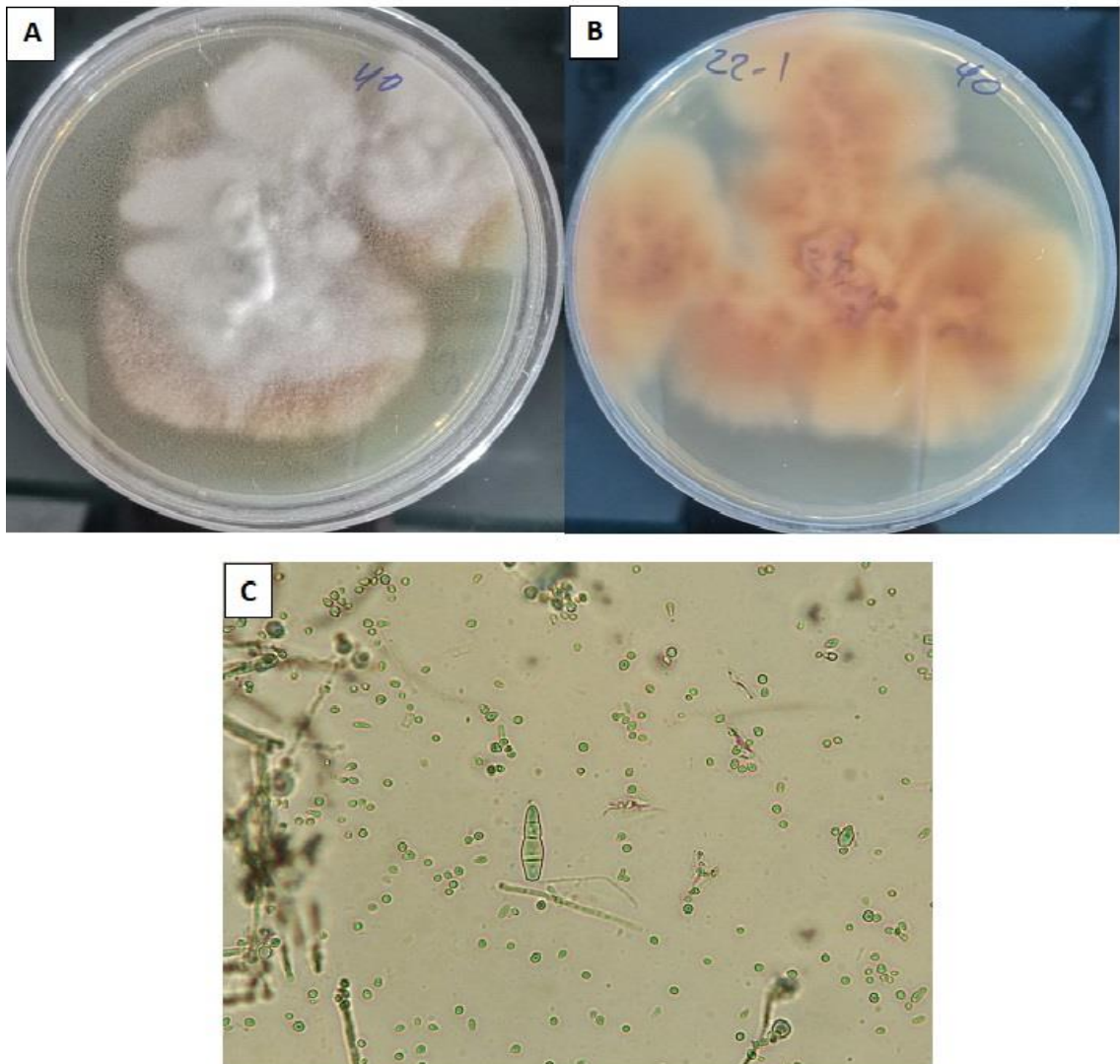


Figure 4.15: Colony of *M. gypseum*

A: Colony in front view, **B:** Colony in reverse view, **C:** Microscopic view

4.3 Antidermatophytic effects of Ag@Cas NPs:

Inhibitory effects of Ag@Cas NPs were identified by the disc diffusion method. Four isolates, including *M. canis*, *T. mentagrophytes-1*, *M. ferrugineum*, and *M. gypseum* were inhibited by all concentrations of Ag@Cas NPs with a great zone of inhibition compared to AgNPs and caspofungin (Figure 4.16). Meanwhile, two isolates of *T. indotineae* were only affected by the higher two concentrations of Ag@Cas NPs (500 and 250) mg/ml. Three isolates (two of *T. indotineae*, and *T. mentagrophytes-2*) were affected by a 500 mg/ml concentration of Ag@Cas NPs with a zone of inhibition of 10.5, 10, and 8.6 mm, respectively. The affected isolates by 250 mg/ml were two isolates of *T. indotineae* (6.4, and 9.3 mm, respectively) (Table 4-2).

The fungus *M. canis* was significantly affected by a low concentration of Ag@Cas NPs (62.5 mg/ml), in which the zone of inhibition was 17.2 mm (Figure 4.16: A). Such significant effects were observed on isolates *T. mentagrophytes-1* and *M. ferrugineum* at a concentration of 250 mg/ml of Ag@Cas NPs (17.6 and 11.25 mm, respectively) (Figure 4.16: B). The isolate *T. mentagrophytes-2* was more resistant to all concentrations of Ag@Cas NPs, except at 500 mg/ml (8.6 mm). This *T. mentagrophytes-2* also observed resistance to the AgNPs and caspofungin. The other two resistant isolates were *T. indotineae-1* and *T. indotineae-2*, which showed resistance to two concentrations of Ag@Cas NPs (125 and 62.5) mg/ml and also to AgNPs and caspofungin (Table 4-2) (Figure 4.16: D). Generally, most isolates were sensitive to prepare nanoparticles (Ag@Cas NPs) more than AgNPs and caspofungin as control.

Table 4-2: Effect of Ag@Cas NPs on isolated fungi using disc diffusion

Method

Isolated fungi	Zone of inhibition (mm)					
	Concentration (mg/ml)					
	500	250	125	62.5	AgNPs	CAS (0.001 mg/ ml)
<i>M. canis</i>	16 ± 2	12 ± 3.1	13.8 ± 1.5	17.2* ± 0.6	9 ± 0.7	9.25 ± 0.5
<i>T. mentagrophytes-1</i>	14.5 ± 3.8	17.6* ± 2.9	12.6 ± 1	12.3 ± 2	13 ± 1.8	–
<i>M. ferrugineum</i>	10.25 ± 1.5	11.25* ± 1.6	7.6 ± 0.5	6 ± 0.6	7.5 ± 2.5	8.6 ± 1
<i>T. indotineae-1</i>	10.5 ± 1.5	6.4 ± 1	–	–	–	–
<i>T. indotineae-2</i>	10 ± 0.6	9.3 ± 0.8	–	–	–	–
<i>T.mentagrophytes-2</i>	8.6 ± 0.4	–	–	–	–	–
<i>M. gypseum</i>	16.6* ± 3	14.8 ± 2	15 ± 1.5	10 ± 1	–	–

Mean ± SD

* :Significant differences at $p < 0.05$

– : Resistance

AgNPs and CAS as control

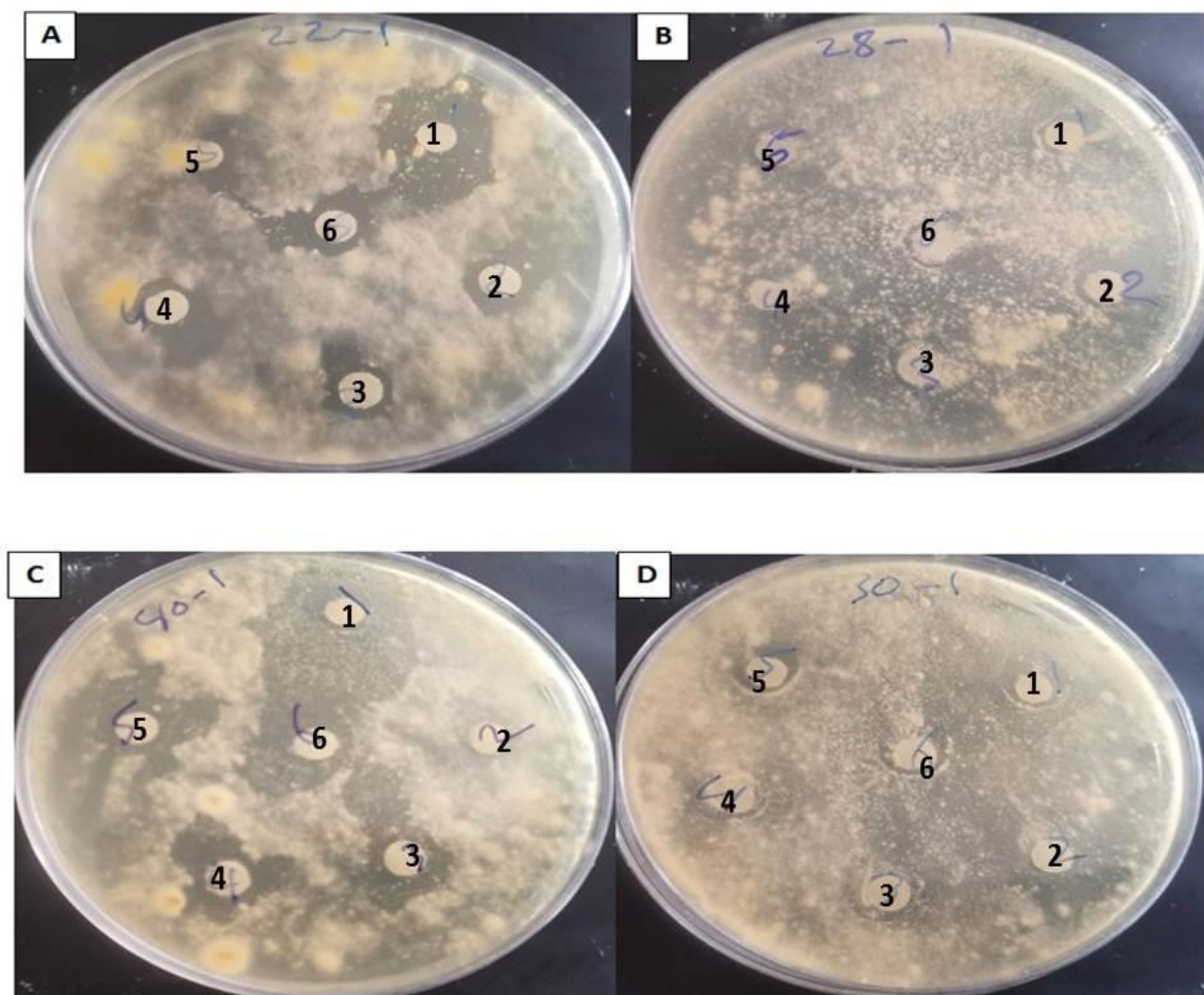


Figure 4.16: Zone of inhibition (mm) of Ag@Cas NPs on (A) *M. canis*
(B) *M. ferrugineum*, (C) *M. gypseum*, (D) *T. indotinea-2*.

The concentration of Cas@AgNPs are: **1:** 500 mg/ml, **2:** 250 mg/ml, **3:** 125 mg/ml,

4: 62.5 mg/ml, **5:** AgNPs, **6:** Caspofungin only.

4.4 Antidermatophytic effects of modified Ag@Cas NPs:

The antidermatophytic action of modified Ag@Cas NPs was evaluated using the disc diffusion method. It was showed less antifungal action against isolated dermatophytes compared to Ag@Cas NPs. Six of seven isolates were inhibited by high concentration 500 mg/ml of modified Ag@Cas NPs. Isolate *T. mentagrophytes-2* was resisted to this high concentration. On the other hand, isolates *M. canis*, *T. mentagrophytes-1*, and *M. gypseum* were inhibited by only 500 mg/ml (10, 13, and 8.4 mm, respectively) (Figure 4-17:A and C). Meanwhile, a concentration of 250 mg/ml affected only *M. ferrugineum* and *T. indotineae-1* (11.5 and 7.5 mm, respectively) (Figure 4.17: B). Isolate *T. indotineae-2* was more susceptible to all concentrations of the modified Ag@Cas NPs (8, 8.5, 7.5, and 7 mm at 500 mg/ml, 250 mg/ml, 125 mg/ml, and 62.5 mg/ml, respectively) (Table 4-3).

Table 4-3: Effect of modified Ag@Cas NPs on isolated fungi using disc diffusion method

Isolated fungi	Zone of inhibition (mm)					
	Concentration (mg/ml)					
	500	250	125	62.5	AgNPs	CAS (0.001 mg/ ml)
<i>M. canis</i>	10 ± 2	–	–	–	9 ± 0.8	9.25 ± 0.4
<i>T. mentagrophytes-1</i>	13 ± 1.4	–	–	–	10.25 ± 1	–
<i>M. ferrugineum</i>	10 ± 0.9	11.25* ± 2.4	–	–	6.5 ± 0.5	7.6 ± 0.7
<i>T. indotineae-1</i>	6.7 ± 0.6	7.5 ± 1	–	–	–	–
<i>T. indotineae-2</i>	8 ± 0.3	8.5 ± 0.8	7.5 ± 0.6	7 ± 0.6	–	–
<i>T.mentagrophytes-2</i>	–	–	–	–	–	–
<i>M. gypseum</i>	8.4 ± 0.4	–	–	–	–	–

Mean ± SD

*: Significant differences at $p < 0.05$

– : Resistance

AgNPs and CAS as control

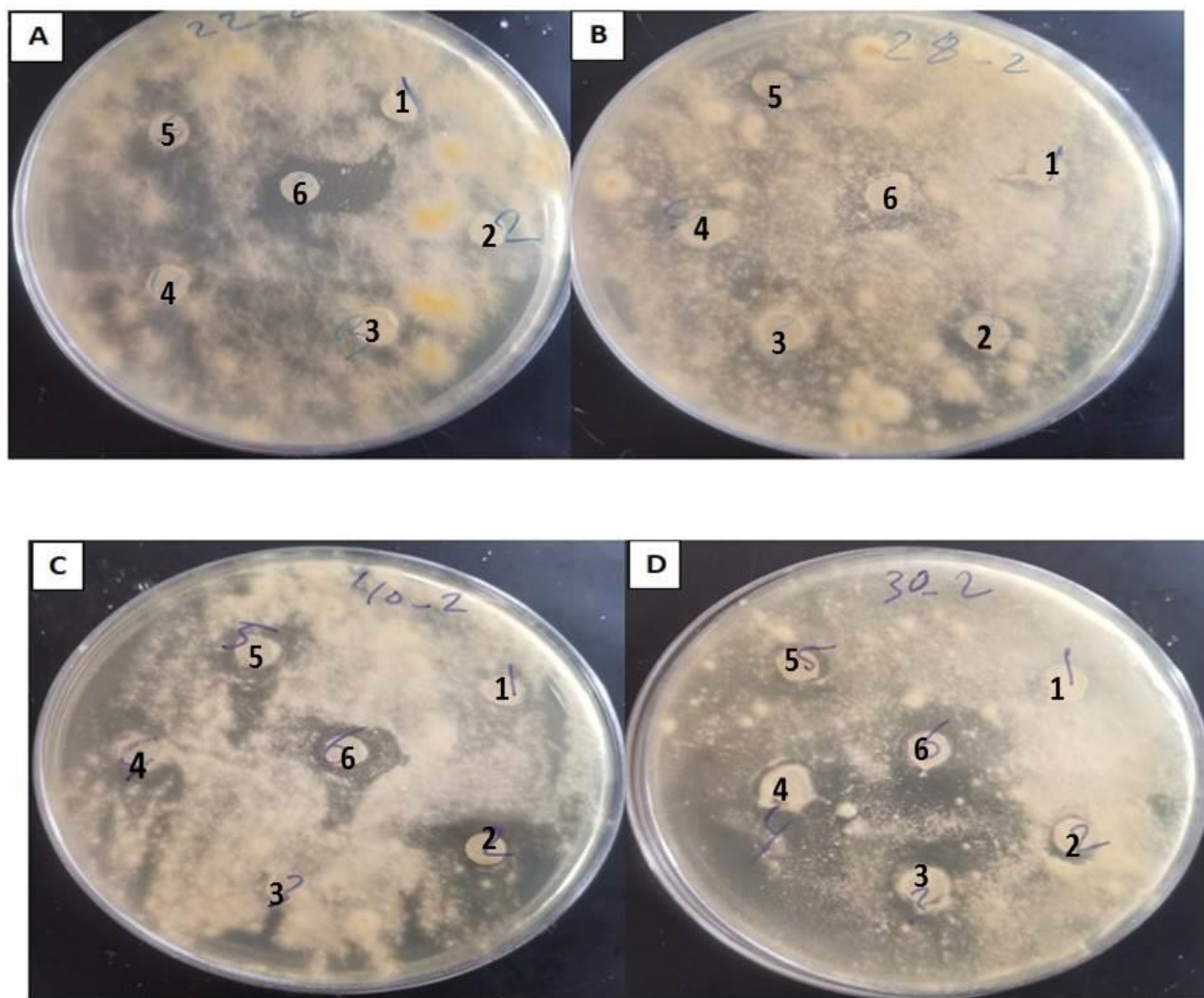


Figure 4.17: Zone of inhibition (mm) of modified Ag@Cas NPs on (A) *M. canis*,

(B) *M. ferrugineum*, (C) *M. gypseum*, (D) *T. indotineae-1*.

The concentration of modified Ag@Cas NPs are: **1:** 500 mg/ml, **2:** 250 mg/ml,

3: 125 mg/ml, **4:** 62.5 mg/ml, **5:** AgNPs, **6:** Caspofungin only

4.5 Minimum inhibitory concentration (MIC) of Ag@Cas NPs on dermatophytes:

The MIC value of Ag@Cas NPs, which showed more antifungal action on isolated dermatophytes than modified Ag@Cas NPs, was determined. *M. canis*, *T. mentagrophytes-1*, *M. ferrugineum* and *M. gypseum* isolates showed inhibition at MIC of 50 mg/ml of Ag@Cas NPs. Isolates *T. indotineae* needed MIC of 20 mg/ml, While isolate *Trichophyton mentagrophytes-2* needed a higher concentration of Ag@Cas NPs to be inhibited (MIC; 500 mg/ml) (Table 4-4).

Table 4-4: Minimum inhibitory concentration (MIC) of Ag@Cas NPs on dermatophytes:

Fungal isolate	MIC (mg/ml)
<i>M. canis</i>	50
<i>T. mentagrophytes-1</i>	50
<i>M. ferrugineum</i>	50
<i>T. indotineae-1</i>	20
<i>T. indotineae-2</i>	20
<i>T. mentagrophytes-2</i>	500
<i>M. gypseum</i>	50

CHAPTER FIVE

DISCUSSION

5.Discussion

5.1 Synthesis and characterization of nanoparticles

5.1.1 Ultraviolet-visible- (UV–vis) spectroscopy analysis

The chemical analysis of Ag@Cas NPs confirmed successful loading of caspofungin on AgNPs. The UV spectra analysis showed that the absorption new peak of Ag@Cas NPs in this study was mean \pm 350-900 nm, an indication of the uploading caspofungin on surface silver. The results of UV-vis spectra of biosynthesized AgNPs that use of cell-free filtrate of *A. niger* revealed strong with a characteristic surface plasmon resonance centered at 420 nm (Al-Hamadani *et al.*, 2017). The Chem-AgNPs and one of Bio-AgNPs produced by *P. chrysogenum* MUM 03.22 revealed a UV spectrum at 430 nm, while the second biosynthetic AgNPs (produced by *A. oryzae* MUM 97.19) had wide spectra (400-550 nm) (Pereira *et al.*, 2014). A preparation of AgNP with an extract of *Phaffia rhodozyma* red yeast had a UV-vis spectrum at 455 nm (Rónavári *et al.*, 2018). The AgNPs with another plant extract (fruit of *Scabiosa atropurpurea* subsp.*maritime*) revealed characterizing of surface plasmon resonance by UV-vis at 423 nm (Essghaier *et al.*, 2022).

5.1.2 Scanning electron microscopy (SEM)

The SEM images of Ag@Cas NPs prepared in the current study had a smoothly spherical shape with a particle size mean \pm 60-150 nm, This size was more effective against dermatophyte and suitable for medical applications. While size of modified Ag@Cas NPs were in μm , its gave less effect. Caspofungin with gold nanoparticles (CAS-AuNPs) in another study also revealed a spherical shape, but with less particle size (20 nm) (Salehi *et al.*, 2021). A large spherical size (100 nm) of AgNPs prepared with growth extract of *T. rubrum* was also described, while AgNPs were aggregated in a ball shape

with a small size (20-50 nm) (Mohsen *et al.*, 2022). Such spherical shape with uniform aggregation of a particle size ranging from 15 to 50 nm was also proven to biosynthesize AgNPs of *A. niger* (Al-Hamadani *et al.*, 2017). Spherical shape, but with variable particle size, was identified for Chem-AgNPs and Bio-AgNPs. The particle size of Chem-AgNPs was 52 nm, while it was in a range of 19-60 nm for Bio-AgNPs (Pereira *et al.*, 2014). A quasi-spherical shape was identified in AgNPs prepared with yeast extract, which has a particle size of 4.1 nm due to they were well separated from each other in minor polydispersity (Rónavári *et al.*, 2018).

5.1.3 Determination of particle size distribution by DLS and Zeta potentials

The particle sizes of prepared nanomaterials in this study were also evaluated by using dynamic laser scattering (DLS) analysis, and they appeared to be greater than those measured by SEM, Because DLS the nanoparticles enter into the solvent and their enlargement, while when examining SEM, they were solid and shrink. Based on Zeta-potentials measurement, the results further approve the successful presence of caspofungin on the silver nanoparticles surface. Such result was also found between DLS and SEM for Chem-AgNPs and Bio-AgNPs (Pereira *et al.*, 2014). In comparison to SEM, DLS measurement showed twofold larger sizes of Bio-AgNPs than Chem-AgNPs. The average size of Chem-AgNPs measured by DLS was 73.72 nm and for Bio-AgNPs was 100.6 nm for those produced by *P. chrysogenum* MUM 03.22 and 76.14 for those from *A. oryzae* MUM 97.19. The CAS-AuNPs characterized by DLS showed nanoparticle size from 30 to 50 nm with good stability based on Zeta-potentials analysis at -38.2 mV (Salehi *et al.*, 2021). Based on DLS analysis, AgNPs with yeast extract showed particle size of 5-9 nm (Rónavári *et al.*, 2018).

5.1.4 Fourier transform infrared spectroscopy FT-IR

The FT-IR analysis in this study confirmed the successful loading of caspofungin on the surface of AgNPs to form Ag@Cas NPs. As a result of the presence of the chemical functional groups in Ag@Cas NPs, the same as the negative caspofungin groups. Both N-H and O-H stretching was confirmed by an absorption of 3361 cm^{-1} . Aromatic and aliphatic C-H stretching were also identified at 2935 cm^{-1} and 2883 cm^{-1} , while bands at 1647 cm^{-1} and 1591 cm^{-1} were attributed to C=O of the acid and amide groups of caspofungin. Close results were also found by Essghaier *et al.* (2022) for AgNPs with fruit extract. FT-IR spectra were noted at 3397 cm^{-1} as an indicator of the stretching of the OH group and at 2361 cm^{-1} of C-H stretching variations. Bands of 1650 , 1379 , and 805 cm^{-1} were also found as stretching variations to C-O, C-C, and C-N, respectively. Al-Hamadani *et al.* (2017) who biosynthesized AgNPs from *A. niger* described a peak of 3421 cm^{-1} that related to the stretch vibration of N-H of primary amides of protein and showed peaks at 2926 cm^{-1} and 2961 cm^{-1} as an indicator to the stretch of C-H of the methylene groups of protein. They also determined that the absorption peak at 2854 cm^{-1} may be assigned to the symmetrical stretch vibration of C-H of alkenes and the band at 1554 cm^{-1} refers to C = C stretch corresponding to an aromatic ring. Chem-AgNPs synthesized by Pereira *et al.* (2014) showed an interaction between silver precursors and PVP by obtaining a band at 1646 cm^{-1} , which represents the C=O group. In the same study, the infrared spectra of both Bio-AgNPs that was produced by *P. chrysogenum* MUM 03.22 and that produced by *A. oryzae* MUM 97.19 presented bands seen at 3220 cm^{-1} , which were assigned to the stretching vibrations of primary and secondary amines, respectively.

5.1.5 X-Ray diffraction (XRD)

The analysis of the X-ray diffraction (XRD) pattern of prepared Ag@Cas NPs in this study confirmed they were less crystalline and more amorphous in

nature which indicated the load of caspofungin on AgNPs, Because caspofungin was an organic compound, the peaks were weak, while AgNPs were an inorganic compound, the peaks were stronger. No obvious sharp peaks were seen in the XRD pattern. This result could be an indicator of the stability of Ag@Cas NPs compared to other nanoparticle preparations of AgNPs in other studies. The XRD analysis of Bio-AgNPs revealed several crystalline peaks at 111, 200, 220, and 311 planes at 2θ angles (Pereira *et al.*, 2014). The AgNPs prepared by Essghaier *et al.* (2022) and Rónavári *et al.* (2018) also showed the same pattern of peaks at the same angles.

5.1.6 Comparison between characteristics of Ag@Cas NPs and modified Ag@Cas NPs

To compare the properties of our forms prepared caspofungin with silver nanoparticles, since the physicochemical properties of the nanocomposites are the main reason for the success of these nanocomposites as therapeutic agents. In the SEM examination, the particle size of the nanocomposite Ag@Cas NPs was smaller than that of the modified Ag@Cas NPs, as it was a nanometer for the Ag@Cas NPs and for the modified Ag@Cas NPs, it was in a micrometer. Also, the results of the DLS examination, showed that the Ag@Cas NPs is smaller than the average size of the modified Ag@Cas NPs.

Caspofungin in the form of caspofungin-silver nanoparticles (Ag@Cas NPs) more antidermatophytic activities than modified Ag@Cas NPs because average particles size of Ag@Cas NPs mean $\pm 60-150$ nm smaller than modified Ag@Cas NPs were larger mean $\pm 0.3-0.5\mu\text{m}$, So its gave less effect. This proves a fact, the small size of NPs has higher antimicrobial activities than larger NPs due to fast entry to the cells.

5.2 Antidermatophytic effects of Ag@Cas NPs

The results of this study showed that Ag@Cas NPs were more effective against most dermatophytic isolates compared to the AgNPs and caspofungin alone. Based on our knowledge, the antifungal effects of caspofungin in nanoparticle form were investigated by only two studies in 2021. The target fungi were species of *Candida*. The first study showed that caspofungin-coated gold nanoparticles (CAS-AuNPs) had more antifungal action on resistance isolates of *C. albicans* and non-albicans *Candida* compared to caspofungin alone (Salehi *et al.*, 2021). The second study examined the effects of caspofungin-zinc oxide nanoparticles on *C. auris*, which is resistant to caspofungin (Fayed *et al.*, 2021). Caspofungin-ZnO NPs revealed more inhibitory action in *C. auris* than caspofungin and also reduced rate of resistant development in this fungus after 10 generations of exposure to caspofungin-ZnO NPs. Furthermore, caspofungin-ZnO NPs were eliminate cross-resistance of *C. auris* to fluconazole.

Caspofungin in the form of caspofungin-silver nanoparticles (Ag@Cas NPs) more antidermatophytic activities than modified Ag@Cas NPs because particles size of modified larger than Cas@AgNPs give less effect .

Caspofungin in our study was prepared in conjugation with silver to obtain a solution of caspofungin-AgNPs and tested its effects on dermatophytes. The AgNPs have been demonstrated to have antidermatophytic effects by several studies. *T. rubrum* was found to be inhibited by 10 µg/ml of AgNPs and the combination of AgNPs with fluconazole and griseofulvin increased the antifungal action of these agents (Noorbakhsh *et al.*, 2011). Three species of dermatophytes, including *M. canis*, *T. mentagrophytes*, and *M. gypseum* were inhibited by AgNPs (Mousavi *et al.*, 2015). Two forms of AgNPs were synthesized; chemical and biological forms (Pereira *et al.*, 2014). The chemical form was synthesized by coating with polyvinylpyrrolidone, while the biological

form was synthesized from the growth extract of two fungi; *Penicillium chrysogenum* MUM 03.22 and *Aspergillus oryzae* MUM 97.19. These forms were evaluated against eight clinical isolates of *T. rubrum*. The chemical form of AgNPs showed more effectiveness on all isolates of *T. rubrum* compared to the biological form. Also it was found that biological form of AgNPs, which was obtained from *P. chrysogenum* MUM 03.22 had more antifungal activities than those from *A. oryzae* MUM 97.19. Mohsen *et al.* (2022) was also prepared biological synthesis AgNPs from the extract of *T. rubrum* culture. This preparation revealed inhibitory action on the growth of *T. rubrum* at concentrations of 100 and 150 mg/ml. *Aspergillus niger* was also used for prepared AgNPs that has antidermatophytic effects on *T. interdigitale* and *E. floccosum* (Al-Hamadani *et al.*, 2017). Free cell extract of the yeast *Phaffia rhodozyma* was used to prepare biological synthesis AgNPs and gold nanoparticles (AuNPs) to use against yeasts and three species of dermatophytes (Rónavári *et al.*, 2018). The used species, *T. mentagrophytes*, *T. tonsurans*, and *M. gypseum* were highly sensitive to synthetic AgNPs and less to AuNPs. Another biological synthesis AgNPs with aqueous extract of *Scabiosa atropurpurea* subsp. *maritima* (L.) fruit also showed antidermatophytic action against *T. rubrum*, *T. interdigitale*, and *M. canis* as well as antibacterial and anti-biofilm of *Candida* spp. (Essghaier *et al.*, 2022). This AgNPs also had the power to eradicate 82% of the biofilm of dermatophytes.

A combination of AgNPs with other materials such as plant extract or conventional antifungals has shown antidermatophytic action. A mixture of AgNPs with leaf extract of *Aloe vera* showed antidermatophytic action against *T. rubrum*, *M. canis*, *T. interdigitale*, and *T. mentagrophytes* (Al-Jobory *et al.*, 2020). The nanoparticles of ketoconazole prepared by mixing with poly-lactic acid nanoparticles showed highly effective antifungal activities against *T. rubrum*, *T. mentagrophytes*, and *M. gypseum* and five species of *Candida* (Endo *et al.*, 2020).

Some isolates of dermatophytes in the present study were inhibited at a high concentration of Ag@Cas NPs. Such high concentration does not eliminate the fact that prepared nanoparticle compounds remain proposed to be new antifungal agents. The AgNPs may show antidermatophytic activities in concentrations higher than conventional antifungals. Griseofulvin showed antifungal action with less concentration than AgNPs on *T. rubrum* (Noorbakhsh *et al.*, 2011), and on *M. canis*, *T. mentagrophytes*, and *M. gypseum* (Mousavi *et al.*, 2015). The mixture of AgNPs with leaves extract of *Aloe vera* required a highly effective concentration (100 µg/ml) to inhibit four species of dermatophytes and the value of inhibition was found to depend on the concentration of AgNPs (Al-Jobory *et al.*, 2020). Such inhibition depending on concentration also found with the antifungal effects of AgNPs prepared from cell-free culture of *T. rubrum* against the growth of *T. rubrum* (Mohsen *et al.*, 2022). The highest effective concentration on the growth of *T. rubrum* was 100 mg/ml and 150 mg/ml, which were considered higher concentrations.

5.3 Minimum inhibitory concentration (MIC) of Ag@Cas NPs on dermatophytes

The results of this study showed that almost all isolates of dermatophytes were inhibited at 50 mg/ml of Ag@Cas NPs. These isolates were resistant to the standard MIC value of pure caspofungin (0.001 mg/ml). Caspofungin with gold nanoparticles in a previous study showed antifungal action on many of *Candida* spp. at MIC (0.06-0.25 µg/ml) which were lower than that of caspofungin (0.12-4 µg/ml) (Salehi *et al.*, 2021). Another preparation of nanoparticle caspofungin with ZnO decreased the effective MIC₅₀ of caspofungin on *C. auris* from 15.47 µg/ml to 10.34 µg/ml (Fayed *et al.*, 2021). However, the high MIC of AgNPs that was required to be used against dermatophytes was also mentioned by many studies. Inhibition of *M. canis*, *T. mentagrophytes* and *M. gypseum* by AgNPs was significantly performed by higher MIC values (200, 180, and 170 µg/ml,

respectively) compared to low MIC of griseofulvin (Mousavi *et al.*, 2015). Species of *M. gypseum*, *T. mentagrophytes* and *T. tonsurans* were inhibited by 30 µg/ml of AgNPs that was prepared from an extract of the yeast *Phaffia rhodozyma* (Rónavári *et al.*, 2018).

Dermatophytes may require a low MIC value of AgNPs to be inhibited. The AgNPs synthesis from the extract of *Scabiosa atropurpurea* subsp. *maritima* (L.) was effective against *T. rubrum* and *T. interdigitale* at MIC 3.9 µg/ml and on *M. canis* at MIC 15.62 µg/ml (Essghaier *et al.*, 2022). Furthermore, this preparation showed fungicidal action on dermatophytes in concentration more than MIC value (MFC; 62.5 µg/ml). Al-Hamadani *et al.* (2017) also found that the fungicidal action of AgNPs prepared from the culture of *A. niger* had a higher value than MIC. *E. floccosum* and *T. interdigitale* which were inhibited by MIC of 0.625 µg/ml and 1.25 µg/ml, respectively, while MFC was 5 µg/ml and 3.54 µg/ml, respectively. The MIC of ketoconazole nanoparticles (0.016, 0.06, and 1.95 µg/ml) was lower than that of ketoconazole (0.06, 0.48, and 7.81 µg/ml) against *T. mentagrophytes*, *T. rubrum*, and *M. gypseum*, respectively (Endo *et al.*, 2020).

The effective MIC of AgNPs in dermatophytes may be variable depending on the nature of preparation. The chemical synthesis AgNPs showed high effectiveness against all clinical isolates of *T. rubrum* at MIC value (0.25 µg/ml to 2.5 µg/ml) which was less than biological synthesis AgNPs (0.5 µg/ml to 5 µg/ml) (Pereira *et al.*, 2014). This study also found that Bio-AgNPs synthesis from *A. oryzae* MUM 97.19 needed higher MIC (7.5 µg/ml) to inhibit dermatophytes than it was by Bio-AgNPs produced by *P. chrysogenum* MUM 03.22 (0.5 µg/ml to 5 µg/ml).

CONCLUSIONS
AND
RECOMMENDATIONS

Conclusions:

1. Seven isolates of dermatophytes were only identified by culturing samples from 100 patients with dermatophytoses.
2. Caspofungin was successfully prepared as nanoparticle forms with silver.
3. Caspofungin in the form of caspofungin-silver nanoparticles (Ag@Cas NPs) has more suitable characteristics as nanoparticles than modified Ag@Cas NPs.
4. The Ag@Cas NPs have more antidermatophytic activities than silver nanoparticles (AgNPs), caspofungin, and modified Ag@Cas NPs.
5. Some isolates of dermatophytes such as *Trichophyton mentagrophytes-2* have resistance to the Ag@Cas NPs.
6. Most isolates were susceptible to low concentrations of Ag@Cas NPs with low MIC.

Recommendations:

- 1-** Stability, pharmacokinetics, and other pharmaceutical studies of Ag@Cas NPs are strongly recommended.
- 2-** An *in vivo* or clinical trials study of Ag@Cas NPs is required.
- 3-** Antifungal activity for other species in future.

REFERENCES

- Abdulkareem, H.A., Khalaf, H. Y. and Mohammed, B. L. (2022).** Epidimological study of dermatophytes infection in kirkuk city. *Annals of R.S.C.B.*, 26(1): 343–352.
- Abed Ali, F.A.H., Al-Janabi, J.K.A. and Alhattab, M.K. (2017).** Prevalence of dermatophyte fungal infection in Hilla, Iraq. *International Journal of ChemTech Research*, 10(6): 827-837.
- Agarwal, M.B., Rathi, S.A., Ratho, N. and Subramanian R. (2006).** Caspofungin: A major breakthrough in treatment of systemic fungal infections. *JAPI*, 54: 943-948.
- Al-Asadi, J. K.K., (2018).** Antimicrobial effect of pyocyanin produced by clinical isolate of *Pseudomonas aeruginosa*. 1-138.
- Alatbee, A.H.D., abdulkareem, E.A. and Obaid, S.A. (2021).** Isolation and identification of dermatophytosis and fungal factors samples from infected patients in basra- iraq. *IMDC-IST*, 1178-1180.
- Al-Hamadani, A.H.U., Al-Muhna, B.M.M. and Abbood, W.S. (2017).** Influence of biosynthesized silver nanoparticles on keratinase activity and mycelial growth of dermatophytesl. *Iraq Med J*, 1(2): 41–47.
- Al-Janabi, A.A.S. (2014).** Dermatophytosis: causes, clinical features, signs and treatment. *Journal of Symptoms and Signs*, 3(3): 200-203.
- Al-Janabi, A.A.S. (2011).** Determination of antidermatophytic effects of non steroidal anti-inflammatory drugs on *Trichophyton mentagrophytes* and *Epidermophyton floccosum*. *Mycoses*. 54:e443-e448.
- Al-Janabi, A.A.S. and Bashi, A.M. (2019).** Development of a new synthetic xerogel nanoparticles of silver and zinc oxide against causative agents

of dermatophytoses. *Journal of Dermatological Treatment*, 0954-6634:1471-1753.

Al-Janabi, A.A.S. and Bashi, A.M. (2022). Synthesis and antifungal activity of novel griseofulvin nanoparticles with zinc oxide against dermatophytic fungi *Trichophyton mentagrophytes* and *Trichophyton verrucosum* :a primary. study. *Current Medical Mycology*, 8(2): 40-44.

Al-Janabi, A.A.H. and Mohamed, J.K. (2021). Dermatophytes isolation from patient with dermatophytosis in Karbala, 2017. *International Journal of Medical Science and Current Research* , 4(3): 655-660.

AlJindan, R. and AlEraky, D.M. (2022). Silver nanoparticles: a promising antifungal agent against the growth and biofilm formation of the emergent *Candida auris*. *Journal of Fungi*, 8(744): 1-9.

Al-Jobory, H.S., Hasan, K.M.A. and Alkaim, A.F. (2020). Antifungal effect of silver nanoparticles on dermatophyte isolated clinical specimens. *Plant Archives*, 20(1): 2897-2903.

Al-Khikani, F.H.O. (2020). Dermatophytosis a worldwide contiguous fungal infection: growing challenge and few solutions. *Biomedical and Biotechnology Research Journal*, 4(2): 117 -122.

Badiee, P, Shokohi, T., Hashemi, J., Mohammadi, R., Najafzadeh, M.J., Shahidi, M.A., Ghasemi, F. and Jafarian, H. (2023). Comparison of *in vitro* activities of newer triazoles and classic antifungal agents against dermatophyte species isolated from iranian university hospitals: a multi central study. *Annals of Clinical Microbiology and Antimicrobials*, 22(15): 1-10.

Balkovec, J. M., Hughes, D.L., Masurekar, P. S, Sable, C.A., Schwartz, R.E. and Singh, S.B. (2014). Reports discovery and development of first in

- class antifungal caspofungin (CANCIDAS®)-a case study. *Natural Product Robert*, 31(1):1-142.
- Bao, Y, Wan, Z. and Li, R. (2013).** *In vitro* antifungal activity of micafungin and caspofungin against dermatophytes isolated from china. *Mycopathologia*, 175: 141–145.
- Bellmann, R. and Smuszkiewicz, P. (2017).** Pharmacokinetics of antifungal drugs: practical implications for optimized treatment of patients. *Infection*, 45: 737–779.
- Bhattacharjee, S. (2016).** DLS and zeta potential – what they are and what they are not?. *Journal of Controlled Release*, 235: 337–351.
- Brescini, L., Fioriti, S., Morroni, G. and Barchies, F. (2021).** Antifungal combinations in dermatophytes. *Journal of Fungi*, 7(727): 1-16.
- Cabañes, F.J. (2020).** Dermatophytes: the names they are a-changin. *Rev Iberoam Micol*, 37(1): 1-2.
- Cappelletty, D. and Eiselstein-McKitrick, K. (2007).** The echinocandins. *pharmacotherapy*, 27(3): 369–388.
- Chen, S.C.A. and Sorrell T.C. (2007).** Antifungal agents. *MJA* , 187(7): 404–409.
- Carmo, P.H.F.d, Garcia, M.T, Figueiredo-Godoi, L.M.A, Lage, A.C.P, Silva, N.S.d. and Junqueira, J.C. (2023).** Metal nanoparticles to combat *Candida albicans* infections: an update. *Microorganisms*, 11(138): 1-19.
- Castillo, H.A.P., Castellanos, L. N.M., Chamorro, R. M., Martínez, R.R. and Borunda, E.O. (2018).** Nanoparticles as new therapeutic agents against *Candida albicans*. *IntechOpen*, 145- 171.

- Datt, S.** and **Datt, T.** (2023). Clinical significance of dermatophytes and their pathogenesis. *Austin Journal of Infectious Diseases*, 10(2): 01-05.
- Endo, E.H., Makimori, R.Y., Companhoni, M.V.P., Ueda-Nakamura, T., Nakamura, C.V. and Filho, B.P.D.** (2020). Ketoconazole-loaded poly-(lactic acid) nanoparticles: characterization and improvement of antifungal efficacy *in vitro* against *Candida* and dermatophytes. *Journal de Mycologie Me´dicale*, 30(101003): 1-6.
- Essghaier, B., Toukabri, N., Dridi, R., Hannachi, H., Limam, I., Mottola, F., Mokni, M., Zid, M.F., Rocco, L. and Abdelkarim, M.** (2022). First report of the biosynthesis and characterization of silver nanoparticles using *Scabiosa atropurpurea subsp. maritima* fruit extracts and their antioxidant, antimicrobial and cytotoxic properties. *Nanomaterials*, 12 (91585):. 1-15
- Fayed, B., Jayakumar, M.N. and Soliman, S.S.M.** (2021). Caspofungin-resistance in *Candida auris* is cell wall-dependent phenotype and potential prevention by zinc oxide nanoparticles. *Medical Mycology*, 59(12): 1243–1256.
- Galliano, I., Dapra, V., Zaniol, E., Alliaudi, C., Graziano, E., Montanari, P., Calvi, C. and Bergallo, M.** (2021). Comparison of methods for isolating fungal DNA. *Practical Laboratory Medicine*, 25. E00221.1-5.
- Gil-Alonso, S., Quindos, G., Canton, E., Eraso, E. and Jauregizar, N.** (2019). Killing kinetics of anidulafungin, caspofungin and micafungin against *Candida parapsilosis* species complex : evaluation of the fungicidal activity *Revista Iberoamericana de Micologa*, 36(1):24–29.
- Gomez-Sequeda, N., Torres, R., and Ortiz, C.** (2017). Synthesis, characterization, and *in vitro* activity against *Candida spp.* of fluconazole

encapsulated on cationic and conventional nanoparticles of poly (lactic-co-glycolic acid). *Nanotechnology, Science and Applications*, 10: 95-104.

Green, M.R. and Sambrook, J. (2001). Molecular cloning: a laboratory manual, 4th edition. *Cold Spring Harbor, New York*, vol 1

Griesser, S.S., Jasieniak, M., Coad, B.R. and Griesser, H.J. (2015). Antifungal coatings by caspofungin immobilization onto biomaterials surfaces via a plasma polymer interlayer. *Biointerphases*, 10(4): 04A307-1 - 04A307-9.

Groll, A. H. and Walsh, T.J. (2001). Caspofungin: pharmacology, safety and therapeutic potential in superficial and invasive fungal infections. *Expert Opinion Investig. Drugs*, 10(8):1545-1558.

Gürsu, B.Y. (2020). Potential antibiofilm activity of farnesol loaded poly(DL-lactide-co-glycolide) (PLGA) nanoparticles against *Candida albicans*. *Journal of Analytical Science and Technology*, 11(43). 1-10.

Hainer, B.L. (2003). Dermatophyte infections. *American Family Physician*, 67(1): 101- 108.

Hsiao, C.R., Huang,L., Bouchara, J. P., Barton,R., ChiehLi, H. and Chang,T.C. (2005). Identification of medically important molds by an oligonucleotide array. *Journal of Clinical Microbiology*, 43(8):3760-3768.

Hashemian, S.M.R., Farhadi, T. and Velayati, A.A. (2020). Caspofungin: a review of its characteristics, activity, and use in intensive care units. *Expert Review of Anti-infective Therapy*, 18(12):1213-1220.

Hindy, N.A.A. and Abiess, A.A. (2019). Isolation and identification of dermatophytes causing dermatophytosis in hilla city, iraq. *Indian Journal of Public Health Research & Development*, 10(10): 2225-2230.

- Hope, W.W.,** Shoham, S. and Walsh, T. (2007). The pharmacology and clinical use of caspofungin. *Expert Opinion. Drug Metab. Toxicol*, 3(2):263-274.
- Huang, T.,** Li, X., Maier, M., O'Brien-Simpson, N.M., Heath, D.E., and O'Connor, A.J. (2023). Using inorganic nanoparticles to fight fungal infections in the antimicrobial resistant era. *Acta Biomaterialia*, 158: 56–79.
- Johnson, M.D.** and Perfect, J. (2003). Caspofungin: first approved agent in a new class of antifungals. *Expert Opinion. Pharmacother*, 4(5):807-823.
- Johnson, L.**(2003). Dermatophytes – the skin eaters. *Mycologist*, 17(4): 147 - 149.
- Kavitha, K.,** Vijaya, N., Krishnaveni, A., Arthanareeswari, M., Rajendran, S., Al-Hashem, A., and Subramania, A. (2020). Nanomaterials for antifungal applications. *Nanotoxicity*, 385-398.
- Kartsonis, N.A.,** Nielsen, J. and Douglas, C.M. (2003). Caspofungin: the first in a new class of antifungal agents. *Drug Resistance Updates*, 6: 197–218.
- Khurana, A.,** Sardana, K. and Chowdhary, A.(2019). Antifungal resistance in dermatophytes: recent trends and therapeutic implications. *Fungal Genetics and Biology*, 132(103255): 1-9.
- Kidd, S.E.** and Weldhagen, G.F. (2022). Diagnosis of dermatophytes: from microscopy to direct PCR. *Microbiology Australia*, 43(1): 9-13.
- Kischkel, B.,** Rossi, S.A., Junior, S.R.S., Nosanchuk, J.D., Travassos, L.R. and Tabora, C. (2020). Therapies and vaccines based on nanoparticles for the treatment of systemic fungal infections. *Frontiers in Cellular and Infection Microbiology*, 10(463): 1-25.

- Kim, K.J., Sang Sung, W., Moon, S.K., Choi, J.S., Kim, J.G., and Lee, D.G.** (2008). Antifungal effect of silver nanoparticles on dermatophytes. *Journal Microbiology Biotechnology*, 18(8): 1482–1484.
- Kofla, G. and Ruhnke, M.** (2011). Pharmacology and metabolism of anidulafungin, caspofungin and micafungin in the treatment of invasive candidosis-review of the literature. *European Journal of Medical Research*, 16: 159-166.
- Kumar, S.** (2006). Organic chemistry spectroscopy of organic compounds. 1-36. <https://docplayer.net/20925190-Organic-chemistry-spectroscopy-of-organic-compounds-prof-subodh-kumar-dept-of-chemistry-guru-nanak-dev-university-amritsar-143005-26-10.html>.
- León-Buitimea, A., Garza-Cervantes, J.A., Gallegos-Alvarado, D.Y., Osorio-Concepción, M. and Morones-Ramírez, J.R.** (2021). Nanomaterial-based antifungal therapies to combat fungal diseases aspergillosis, coccidioidomycosis, mucormycosis, and candidiasis. *Pathogens*, 10(1303): 1-22.
- Letscher-Bru, V. and Herbrecht, R.** (2003). Caspofungin: the first representative of a new antifungal class. *Journal of Antimicrobial Chemotherapy*, 51: 513–521.
- Malathi, S., Manikandan, D., Nishanthi, R., Jagan, E.G., Riyaz, S.U.M., Palani, P., and Simal-Gandara, J.** (2022). Silver nanoparticles, synthesized using *Hyptis suaveolens* (L) Poit and their antifungal activity against *Candida* spp. *ChemistrySelect*, 7: 1-11.
- Malik, M., Chan, K. H. and Azimi, G.** (2021). Quantification of nickel, cobalt, and manganese concentration using ultraviolet-visible spectroscopy†. Quantification of nickel, cobalt, and manganese concentration using ultraviolet-visible spectroscopy. *RSC Adv.* 11: 28014-28028.

- McCormack, P.L.** and Perry, C.M. (2005). Caspofungin a review of its use in the treatment of fungal infections. *Adis Drug Evaluation*, 65 (14): 2049-2068.
- Martinez-Rossi, M.N.,** Bitencour, T.A., Peres, N.T. A., Lang, E. A. S., Gomes, E.V., Quaresimin, N.R., Martins, M.P., Lopes, L. and Rossi, A. (2018). Dermatophyte resistance to antifungal drugs: mechanisms and prospectus. *Frontiers microbiology*, 9(1108): 1-18.
- Mehta, B.K.,** Chhajlani, M. and Shrivastava, B.D. (2017). Green synthesis of silver nanoparticles and their characterization by XRD. *J. Phys.*,836: 1-4.
- Mohammed, S.J.,** Noaimi, A.A. and Sharquie, K.E. (2015). A Survey of dermatophytes isolated from Iraqi patients in Baghdad city. *AL-Qadisiya Medical Journal*, 11(19): 10-15.
- Morovat, T.,** Bahram, F., Mohammad, E., Setareh, S. and Mehdi, F. M. (2009). Distribution of different carbapenem resistant clones of *Acinetobacter baumannii* in Tehran Hospitals. *New Microbiologica*, 32: 265-271.
- Mohsen, L. Y.,** Alsaffar, F., Lilo, A. and Al-Shamari, K. (2022). Silver nanoparticles that synthesis by using *Trichophyton rubrum* and evaluate antifungal activity. *Archives of Razi Institute*, 77(6): 2145-2149.
- Mousavi, S. A.A.,** Salari, S. and Hadizadeh, S. (2015). Evaluation of antifungal effect of silver nanoparticles against *Microsporium canis*, *Trichophyton mentagrophytes* and *Microsporium gypseum*. *Iran J Biotech*, 13(4): 38-42.
- Nagaraj, S.,** Manivannan, S. and Narayan, S. (2021). Potent antifungal agents and use of nanocarriers to improve delivery to the infected site – a systematic review. *Journal of Basic Microbiology*, 61(10): 849-873.

- Najem, M.H., Al-Salhi , M.H. and Hamim, S.S. (2016).** Study of dermatophytosis prevalence in Al-Nassiriyah city- Iraq. *World Journal of Pharmaceutical Sciences*, 4(4): 166-172.
- Nayak, S., Bhat, M.P., Udayashankar, A.C., Lakshmeesha, T.R., Geetha, N. and Jogaiah, S. (2020).** Biosynthesis and characterization of *Dillenia indica* - mediated silver nanoparticules and their biological activity. *Appl. Organomet. Chem*, 34(4): 1-9.
- Noorbakhsh, F., Rezaie, S., Shahverdi, A.R. (2011).** Antifungal Effects of Silver nanoparticle alone and with combination of antifungal drug on dermatophyte pathogen *Trichophyton rubrum*. International Conference on Bioscience, *Biochemistry and Bioinformatics*, 5: 364-367.
- Nweze, E.I., Mukherjee, P.K., and Ghannoum, M.A. (2010).** Agar-based disk diffusion assay for susceptibility testing of dermatophytes, *Journal of Clinical Microbiology*, 48(10):3750-3752.
- Paryuni, A.D., Indarjulianto S. and Widyarini S. (2020).** Dermatophytosis in companion animals: A review. *Veterinary World*, 13(6): 1174-1181.
- Pfaller, M. A, Boyken, L. Hollis, R.J, Messer, S.A, Tendolkar, S. and Diekema D.J. (2006).** *In vitro* susceptibilities of *Candida spp.* to caspofungin: four years of global surveillance. *Journal of Clinical Microbiology* , 44(3): 760–763.
- Pacifici, G.M. (2020).** Clinical pharmacology of caspofungin in infants and children. *Journal of Clinical Pharmacology and Therapeutics*, 1(1006): 023-031.
- Perlin, D.S. (2015).** Mechanisms of echinocandin antifungal drug resistance. *Annala of the New York Academy Sciences*, 1354: 1-11.

- Perween,** Khan, H.M., and Nusrat, N.F. (2019). Silver nanoparticles: an upcoming therapeutic agent for the resistant *Candida* infections. *Journal of Microbiology & Experimentation*, 7(1): 49–54.
- Pereira,** L., Dias, N., Carvalho, J., Fernandes, S., Santos, C., Lima, N. (2014). Synthesis, characterization and antifungal activity of chemically and fungal- produced silver nanoparticles against *Trichophyton rubrum*. *Journal of Applied Microbiology*, 117: 1601—1613.
- Qureshi,** A.T. (2013). Silver nanoparticles as drug delivery systems. Louisiana State University Doctoral Dissertations, 1-154.
- Rippon,** J.W. (1988). Medical mycology. W.B. Saunders. Philadelphia. 1988,pp 258- 266.
- Rocha,** C.H.L., Rocha, F.M.G., Bitencourt,T.A., Martins,M.P., Sanches,P.R., Rossi,A. and Martinez-Ross,N.M. (2022). Synergism between the antidepressant sertraline and caspofungin as an approach to minimise the virulence and resistance in the dermatophyte *Trichophyton rubrum*. *Journal of Fungi*, 8(815): 1-13.
- Rónavári,** A., Lgaz, N., Gopisetty, M.K., Szerencsés, B., Kovács, D., Papp, C., Vágvölgyi, C., Boros, I.M., Kónya, Z., Kiricsi, N. and Pfeiffer, I. (2018). Biosynthesized silver and gold nanoparticles are potent antimycotics against opportunistic pathogenic yeasts and dermatophytes . *International Journal of Nanomedicine*, 13: 695–703.
- Rouzaud,** C., Hay R., Chosidow, O., Dupin, N., Puel A., Lortholary, O. and Lanternier, F. (2016). Severe dermatophytosis and acquired or innate immunodeficiency: a review. *J. Fungi*, 2(4): 1-13.
- Sabir,** S., Arshad, M., Ilyas, N., Naz, F., Amjad, M., Malik, N., and Chaudhari,S. (2022). Protective role of foliar application of green

synthesized silver nanoparticles against wheat strip rust disease caused by *Puccinia striiformis*. *Green Processing Synthesis*, 11(1), 29-43.

Salehi, Z., Fattahi, A., Lotfali, E., Kazemi, A., Shakeri-Zadeh, A., and Nasrollahi, S.H. (2021). Susceptibility pattern of caspofungin-coated gold nanoparticles against clinically important *Candida* species. *Advanced Pharmaceutical Bulletin*, 11(4): 693-699.

Sharquie, K.E. and Jabbar, R.I. (2021). Major outbreak of dermatophyte infections leading into imitation of different skin diseases: *Trichophyton mentagrophytes* is the main criminal fungus. *J Turk Acad Dermatol*, 15(4):91-100.

Shweta and Manju. (2018). Dermatophytosis and its clinical types. *Journal of Emerging Technologies and Innovative Research*, 5(11): 2349-5162.

Soliman, G.M. (2017). Nanoparticles as safe and effective delivery systems of antifungal agents: achievements and challenges. *International Journal of Pharmaceutics* 523:15–32.

Song, J.C. and Stevens, D.A. (2015). Caspofungin: pharmacodynamics, pharmacokinetics, clinical uses and treatment outcomes. *Critical Reviews in Microbiology*, *Early Online*: 1–34.

Stone, E.A., Fung, H.B. and Kirschenbaum, H.L. (2002). Caspofungin: an echinocandin antifungal agent. *Clinical Therapeutics*, 24(3): 351-377.

Sucher, A.J., Chahine, E.B. and Balcer, H.E. (2009). Echinocandins: the newest class of antifungals. *The Annals of Pharmacotherapy*, 43:1647-1657.

Suganthi, M. (2017). Pathogenesis and clinical significance of dermatophytes: a comprehensive review. *Innovations in Pharmaceutics and Pharmacotherap*, 4(1): 62-70.

- Su, H., Jiang, W, Verweij, P. E., Li, L., Zhu, J., Han, J., Zhu, M. and Deng, S.** (2023). The *in vitro* activity of echinocandins against clinical *Trichophyton rubrum* isolates and review of the susceptibility of *T. rubrum* to echinocandins worldwide. *Infection and Drug Resistance*, 16: 5395–5403.
- Szymanski, M., Chmielewska, S., Czyzewska, U., Malinowska, M. and Tylicki, A.** (2022). Echinocandins – structure, mechanism of action and use in antifungal therapy. *Journal of Enzyme Inhibition and Medical Chemistry*, 37(1): 876–894.
- Wiederhold, N.P. and Herrera, L.A.** (2012). Caspofungin for the treatment of immunocompromised and severely ill children and neonates with invasive fungal infections. *Clinical Medicine Insights: Pediatrics*, 6 :19–31.
- Xia, Z.K., Ma, Q.H., Li, S.Y., Zhang, D.Q., Cong, L., Tian, Y.L. and Yang, R.Y.** (2016). The antifungal effect of silver nanoparticles on *Trichosporon asahii*. *Journal of Microbiology, Immunology and Infection*, xx: 1-7.
- Yamada, S. M., Tomita, Y., Yamaguchi, T. and Matsuki, T.** (2016). Open access micafungin versus caspofungin in the treatment of *Candida glabrata* infection: a case report. *Journal of Medical Case Reports*, 10(316): 1-5.
- Zhang, C, Cheng, J. Jiang, Y. and Liu, j.** (2014). Application of caspofungin in china compared with amphotericin B and fluconazole. *therapeutics and Clinical Risk Management*, 10:737–741.

الخلاصة:

ان مرض سعفة الجلد هو اصابة فطرية ذات نسبة حدوث وتكرار عالي تسببها فطريات السعفة. كاسبوفنجين كواحد من الايكانوكاندين يعد احد المرشحين كعلاج فعال لفطريات السعفة. تم تقييم فعالية اثنين من أشكال الجسيمات النانوية المحضرة من الكاسبوفونجين والفضة، جسيمات الكاسبوفونجين والفضة النانوية وجسيمات الكاسبوفونجين والفضة النانوية المعدل، في المختبر في هذه الدراسة ضد فطريات السعفة، وتم تحليل الخصائص الكيميائية لهذه المستحضرات باستخدام المجهر الإلكتروني الماسح (SEM)، وتشتت الضوء الديناميكي (DLS) مع إمكانات زيتا والتحليل الطيفي للأشعة فوق البنفسجية والمرئية (UV-vis) والتحليل الطيفي للأشعة تحت الحمراء (FT-IR)، وحيود الأشعة السينية (XRD).

سبعة أنواع من الفطريات الجلدية تتضمن ثلاث انواع من جنس *Microsporum* واربعة انواع من جنس *Trichophyton* تم عزلها من 7 مرضى (3 ذكور و4 إناث) مع أنواع مختلفة من الاصابات بسعفة الجلد، اذ تم تشخيص الأنواع على أساس الصفات المظهرية والتحليلات الجزيئية باستخدام جينات *ITS1* و *ITS2*. تم تقييم الأنشطة المضادة للفطريات لأشكال الجسيمات النانوية المعدلة حديثاً باستخدام طريقة الانتشار من القرص، كما تم تحديد الحد الأدنى للتركيز المثبط بواسطة طريقة تخفيف المرق.

بناءً على التحليل الكيميائي لأشكال جسيمات الكاسبوفونجين النانوية، امتلك شكل جسيمات الكاسبوفونجين والفضة النانوية خصائص أكثر ملاءمة كجسيمات متناهية الصغر مقارنة مع جسيمات الكاسبوفونجين والفضة النانوية المعدل، وكانت أطياف الأشعة فوق البنفسجية الى جسيمات الكاسبوفونجين والفضة النانوية عند 350-900 نانومتر. كان لدى جسيمات الكاسبوفونجين والفضة النانوية شكل كروي متخذ طبقة خارجية حول جسيمات الزئبق النانوية بحجم أصغر من جسيمات الكاسبوفونجين والفضة النانوية المعدلة. اعتماداً على تشتت الضوء الديناميكي، كان حجم جسيمات الكاسبوفونجين والفضة النانوية أعلى من ~ 100 نانومتر إلى ~ 250 نانومتر مقارنة مع جسيمات الزئبق النانوية وجسيمات الكاسبوفونجين والفضة النانوية المعدلة أعلى (400 نانومتر). تم تحديد مختلف الروابط الكيميائية في جسيمات الكاسبوفونجين والفضة النانوية بواسطة التحليل الطيفي للأشعة تحت الحمراء وحيود الأشعة السينية كمؤشر لتحميل الكاسبوفونجين على سطح جسيمات الزئبق النانوية.

أظهرت جسيمات الكاسبوفونجين والفضة النانوية تأثيرات مضادة للفطريات على فطريات السعفة مقارنةً مع جسيمات الزئبق النانوية أو الكاسبوفونجين وحده. تم تثبيط جميع العزلات بواسطة جسيمات الكاسبوفونجين والفضة النانوية عند التراكيز 250 و500 ملغرام/مل. تم تثبيط العزلات *M. canis*, *T. mentagrophytes-1*, *M. ferrugineum*, و *M. gypseum* مع منطقة تثبيط عالية وبتراكيز منخفض (62.5) ملغرام/مل من جسيمات الكاسبوفونجين والفضة النانوية (17.2، 12.3، 6 و 10 ملم، على التوالي).

احتاجت العزلات *Trichophyton indotineae* إلى تركيزات عالية من جسيمات الكاسبوفنجين والفضة النانوية لتثبط.

تم تحديد الحد الأدنى للتركيز المثبط الى جسيمات الكاسبوفنجين والفضة النانوية عند 50 ملغرام /مل لاربع عزلات. اما عزلة *Trichophyton indotineae* الحد الادنى للتركيز المثبط بقيمة 20 ملغرام /مل. العزلة *Trichophyton mentagrophytes-2* احتاجت إلى الحد الأدنى للتركيز المثبط بقيمة 500 ملغرام /مل، ومن ناحية أخرى، كان تأثير جسيمات الكاسبوفنجين والفضة النانوية المعدلة على فطريات السعفة أقل من جسيمات الكاسبوفنجين والفضة النانوية، إذ ان فعالية جسيمات الكاسبوفنجين والفضة النانوية كانت فعالة عند التركيز العالي (50) ملغرام /مل على ستة من سبع عزلات. كانت العزلة *Trichophyton mentagrophytes-2* مقاومة لهذا التحضير النانوي، في حين كانت العزلة *Trichophyton indotineae* 2 أكثر حساسية.

الاستنتاجات: يحتوي الكاسبوفونجين في شكل Ag@Cas NPs على أنشطة مضادة للفطريات الجلدية أكثر من الجسيمات النانوية الفضية (AgNPs)، والكاسبوفونجين، وAg@Cas NPs المعدلة.



جمهورية العراق

وزاره التعليم العالي والبحث العلمي

جامعة كربلاء كلية الطب

فرع الاحياء المجهرية

التأثير المختبري لجسيمات الكاسبوفونجين-الفضة النانوية على فطريات السعفة

رسالة مقدمة الى

مجلس كلية الطب جامعة كربلاء

كجزء من متطلبات نيل شهادة الماجستير في الاحياء المجهرية الطبية

من قبل الطالبة

سرى حميد محمد خضران الزبيدي

جامعة كربلاء- كلية العلوم- بكالوريوس علوم حياة (2008)

بإشراف

الاستاذ الدكتور علي عبد الحسين صادق الجنابي

الاستاذ المساعد الدكتور اثير حميد عوده الغانمي